FORMATION OF PLANETARY SYSTEMS BY SUCCESSIVE CONTRACTIONS OF THE SOLAR NEBULA

I: *A General Survey of this Theory and First Applications*

V. DYCZMONS

Theoretical Chemistry Group, University of Göttingen, Federal Republic of Germany

(Received 15 August, 1977)

Abstract. The theory discussed in the present paper is a solar nebula-type theory which assumes the initial existence of a big disk-shaped gas cloud in rotational motion around the Sun. At the outer edge of the gas cloud there is a steady loss of angular momentum, which is mainly caused by the diffusion induced by turbulence and shock waves. This leads to the formation of a doughnut-shaped gas ring at the edge of the cloud, outside of which there is plasma in a state of partial corotation. The gas ring is then slowly shifted towards the Sun, whereby the grains of solid matter within the gas cloud are also transported and collected within the gas torus. During the contraction process the following two situations arise: First, due to the small amount of friction, the angular momentum of the inner part of the ring rapidly exceeds that of the outer part. Second, the angle between the orbits of the inner and outer part of the gas ring increases gradually. When, during contraction, a certain distance is covered, the gas ring turns over, i.e. there is a sudden interchange of the inner and outer parts of the gas ring, where two adjacent rings of solid matter (jet streams) are formed. Immediately after the turn-over process the speed of contraction is at first drastically reduced, but then the gas ring is shifted once more towards the Sun. This process is then repeated periodically. The planets originate from the outer rings of solid matter, which contain much more matter than their adjacent inner rings. The inclination between the inner and outer rings is roughly 5°. In particular, Mercury, the Moon, Titan as well as Triton result from the innermost rings of matter. Having gone through the formation process, most of the planets acquire a rotating gas disk out of which the regular satellites are also created by the same periodic contraction process (hetegonic principle). This theory is the first that can explain all noteworthy facts about our planetary system and the satellite systems in a qualitative yet conclusive way.

1. Introduction

A good survey of the currently existing theories and problems in this field is given by the papers presented at the Nice Symposium (1972) and by Alfvén and Arrhenius (= A and A) (1973). The most essential data on the planets and satellites can be found in Allen's book (1973), in the book of A and A (1975) and by Newburn and Gulkis (1973); further, in the physico-chemical investigations of Lewis (1972a, b), Anders (1971) and Brecher (1972). Among the comprehensive theories there are only a few still under discussion (see Nice Conference, 1972). All other theories (at present about 45) are at least partially disproved and most of them explain only a small portion of the known data.

At present there still exists a considerable amount of data which have not yet been explained satisfactorily. These facts are, in particular:

1. The orientation of the rotational axes of the individual planets.

The Moon and the Planets **18** (1978) 105–142.

2. The correct sequence of the orbital distances of planets and satellites, which is more precise than a geometric series.
3. The correct sequence for the spin periods of the planets.
4. The orbits of the planets Mercury and Pluto as well as the orbit of the asteroid Pallas (Whipple *et al.*, 1972).
5. The problem why only Venus rotates in a retrograde direction and why, among the larger satellites, only Triton moves around Neptune in a retrograde direction.
6. If one compares the three regular satellite systems (Jupiter, Saturn and Uranus) to each other and each to the planetary system, one sees that the average R_{i+1}/R_i-values of the four individual systems are different; here R_i is the distance of the ith satellite (planet) from the central body. Why is there just this given order of the average R_{i+1}/R_i-values?
7. Why are the satellite systems nearly planar in contrast to the planetary system?
8. A rough estimate of mass ratios between the different planets and between the planets and their satellites should be predictable.
9. Why do we only have the two associated large bodies, Triton and Pluto, with its unusual rotation period for the outermost planet, Neptune?
10. The precise formation of the Moon. Why does it have more high temperature condensates than the Earth and a relatively high mass? What caused its intense cratering to take place 4.1–4.6 billion years ago? (cf. Schmitt, 1975).

One would not expect, within the scope of a solar nebular theory, any theory which can precisely compute all known data, because the radial mass distribution within the disk is not exactly known. In spite of this difficulty, this new theory leads to unexpected but reasonable results due to the following favourable factors:

1. Only a rough initial radial dependence of the mass distribution is needed to get all the essential facts.
2. There is only a single well-defined process which repeats itself again and again.
3. This process depends mainly on the distance from the central body.

Like A and A we also emphasize that a theory of the formation of secondary bodies around central bodies (hetegonic principle) is needed. Because the fundamental process of this theory is very complex, a simplified description is often given in this paper.

2. Prerequisites for this Theory

Only a few requirements are necessary for the formation of secondary bodies:

1. On the outer edge of the hetegonic disk (= circumsolar gas disk or circumplanetary gas disk) we assume the temperature to be high enough for a diffusion current of H_2 away from the central body.

2. A diameter of the solar or planetary nebula (= hetegonic nebula) of at least twice the orbital diameter of the outermost secondary body.
3. The initial mass of the hetegonic nebula should be about $0.05M_c$, where M_c is the mass of the central body. In the case of our planetary system, we further assume that the initial radial distribution function $f(R) = 2\pi R^2 \int_{-\infty}^{+\infty} \varrho(R, h)\, \mathrm{d}h$ of mass within the disk had a maximum of between 4 and 7 AU, where ϱ is the mass density. Further, we assume that originally within the circumsolar nebula the distribution of element abundances was the same as in the Sun (cf. Urey, 1972).

3. Hypotheses for the Radial Density Distribution in the Solar Nebula

The following processes are speculative, but their purpose is only to make our starting point plausible. At the outset there was a slowly rotating collapsing gas cloud with a mass of about 1.05 $M_\odot$. We suggest that there are (at least) three possible explanations to get the radial density distribution which we have proposed (see Table II).

1. Angular momentum transfer from the newly formed proto-Sun by means of its high magnetic field to the plasma in its surroundings. Here we suggest, according to A and A (1973), that matter was still being collected from the periphery of the original gas cloud. It was stopped and became ionized when falling towards the Sun. In contrast to A and A, we assume that this phase lasted only 10^5–10^6 years. So we only 'partly' get a band structure (cf. A and A, 1974). Thereafter the plasma condenses rapidly.
2. Already during the contraction of the cloud there is a steady transport of spin angular momentum from its blob to 'infinity' by Alfvén waves, as suggested by Mestel (1972).
3. There was a T Tauri phase of the proto-Sun before the planets' accumulation. In contrast to most other theories (see, e.g. Cameron, 1973) it is very unlikely that the solar nebula was swept away by the onset of the T Tauri stage as Handbury and Williams (1976) have shown. During the T Tauri phase the proto-Sun lost most of its angular momentum.

4. Properties of a Hetegonic Gas Disk

4.1. Laws of Motion

In a central gravitational field of a mass M_c the motion of a solid body which moves on a circular orbit is determined by Kepler's third law: i.e.,

$$v_{\mathrm{K}}(R) = \sqrt{\gamma M_c/R}; \qquad \omega_{\mathrm{K}}(R) = R^{-1} v_{\mathrm{K}}(R); \qquad C_{\mathrm{K}}(R) = R v_{\mathrm{K}}(R). \tag{1}$$

The motion of the gas is, moreover, determined by grad p. Without turbulence we get (cf. Equation (17))

$$v_G(R) = [v_{\mathrm{K}}^2(R) + R\varrho^{-1}\,\mathrm{grad}\,p]^{1/2}. \tag{2}$$

Therefore, if there is no turbulence and grad p is small, the difference in velocity between a solid body and the gas can be approximated as

$$\Delta v = v_G(R) - v_K(R) \approx 0.5\omega_K^{-1}(R)\varrho^{-1} \operatorname{grad} p. \tag{3}$$

In addition to the central gravitational field of the central body, there is the small gravitational field of the hetegonic disk itself. But, for most purposes, one can neglect its gravitational influence.

4.2. Turbulence

One of the most interesting topics in most of the solar nebula type theories is the question of whether or not turbulence occurs within the gas disk. Normally, the magnitude of the Reynolds number (where η_v is the coefficient of viscosity and L is a characteristic length)

$$Re = \eta_v^{-1}\varrho v L \tag{4}$$

will answer this question. The critical value for this case is estimated by ter Haar (1972) to be in the order of 10^7, which means turbulence will occur. But the Reynolds number cannot be a reliable criterion since it would also suggest turbulence in the case where $v(R) \sim R$ (i.e. $\omega = \text{const.}$). But this makes no sense because the gas would then be moving like a rigid disk. Our criteria is: do small radial displacements cause an energy gain or do they not. To see this we take two gas elements with unit mass both in circular motion, one with radius R and angular momentum $C_G(R)$ and the other with radius $R + \mathrm{d}R$ and angular momentum $C_G(R + \mathrm{d}R)$. Exchange of both gas elements from one orbit to the other gives the change of energy $\mathrm{d}E$ as

$$\mathrm{d}E = R^{-1}\left[\frac{\mathrm{d}}{\mathrm{d}R} C_G^2(R)\right](\mathrm{d}R/R)^2. \tag{5a}$$

There is only an energy gain if $\mathrm{d}E$ is negative, i.e. $C_G'(R) < 0$. This means that if $C_G'(R) > 0$ then the system is stable against small perturbations and turbulence does not occur. According to Equation (5a), we take as a measurement for the intensity of turbulence

$$W(R) \sim R^{-1}\left[\frac{\mathrm{d}}{\mathrm{d}R} C_G^2(R)\right]. \tag{5b}$$

Because of the small gradient of gas pressure, rotation becomes nearly Keplerian. By means of (1) and (5b) we see that there is no turbulence, and this seems to be acceptable. In this theory it is not important whether or not turbulence occurs in a hetegonic disk, whereas relation (5b) is of great interest.

4.3. Barometric equation

The decrease in gas density with an increase in the distance h from the central plane is given by the following considerations: The gravitational force of the central body which acts on the gas at some distance h from the central plane and at a distance R from the central body is given by

$$K_r = -\gamma M_c h(R^2 + h^2)^{-1.5}. \tag{6}$$

Because the gas consists mainly of H_2 and He, it is in good approximation an ideal gas. If we assume a constant temperature T (cf. Section 5.6) for a fixed R-value, we get, with $\varrho = \varrho_0 * p/p_0$ the 'barometric equation' (in M.K.S. units),

$$\varrho(h) = \varrho(0) \exp\left[-\frac{\gamma M_c \varrho_0 T_0}{2R_G p_0}\frac{1}{RT}(1 - (1 + (h/R)^2)^{-0.5})\right], \tag{7a}$$

where ϱ_0 is the average density for p_0 and T_0, and R_G is the gas constant. A good approximation for Equation (7a) is given by (see also Safronov, 1972)

$$\varrho(h) = \varrho(0) \exp[-4.013 \times 10^{-15}\bar{m}M_c(RT)^{-1}(h/R)^2], \tag{7b}$$

where we have used M.K.S. units and $\bar{m}$ is the average molecular weight. When turbulence occurs the scale height of the disk is, of course, much greater.

4.4. Importance of Friction within the Gas Disk

Let us consider a cube of 1 m^3 of the gas in a circular orbit with radius R. Two planes of this cube should be perpendicular to the radial vector $\vec{R}$. For a laminar current the friction which acts on the inner plane A is given by (in M.K.S. units)

$$F(R - \tfrac{1}{2}) = \eta_v A v'_{\mathrm{K}}(R) = \eta_v \cdot 1\ \mathrm{m}^2(-0.5\omega_{\mathrm{K}}(R - 0.5)). \tag{8}$$

On the outer plane we have the friction $F(R + \frac{1}{2})$. The whole force of friction which acts on the cube is then given by

$$\Delta K = F(R + \tfrac{1}{2}) - F(R - \tfrac{1}{2}) = 0.75\eta_v\omega_{\mathrm{K}}(R)/R. \tag{9}$$

The speed variation within the time t is given by

$$\Delta v_F = K(t/\varrho). \tag{10}$$

For example, within 10^6 years we get, for the Earth orbit, $T = 100$ K, $\bar{\varrho} \approx 3 \times 10^{-5}$ kg m^{-3}, $\eta_v \approx 10^{-5}$ kg m^{-1} s^{-1}; for the variation in velocity, $\Delta v = 1 \times 10^{-5}$ m s^{-1}; and for the orbit of Neptune, accordingly, $\Delta v \approx 3 \times 10^{-4}$ m s^{-1}.

The small change of the orbital velocity accounts for the fact that there is neither a transport of angular momentum nor a shifting of the gas in the radial direction by means of friction. Also, if we assume that there is turbulence, which means η_v is greater (say, by a factor of 10^3), then this statement also remains valid.

4.5. Plasma within the Gas Disk

After a short cooling phase of the newly formed hetegonic disk the temperature is relatively low (40–300 K). Looking at the Hartmann number (cf. ter Haar, 1972), one sees that there is no plasma because the gas density is too high and the temperature is too low.

5. General Survey of this Theory

5.1. Loss of Angular Momentum at the Edge of the Gas Disk

In the beginning we have a loss of angular momentum at the edge of the disk. Due to diffusion, H_2-molecules, He and H-atoms escape. The velocity $\vec{v}_e$ of a molecule in the gas is composed of two vectors (see Figure 2, $\bar{\delta} = 0$): the velocity of the centre of gravity of the gas $\vec{v}_G$ (cf. Equation (2)) and the velocity $\vec{v}_M$ of the molecules with respect to the centre of gravity. The distribution of v_M with regard to the molecules is given by the Maxwellian velocity distribution

$$w(\lambda, u) = \frac{4}{\sqrt{\pi}} \lambda^{1.5} u^2 \exp(-\lambda u^2); \qquad \lambda = m/2kT. \tag{11}$$

The relative number $N(u_0)$ of molecules whose velocity is larger than u_0 is given by

$$N(\lambda, u_0) = \int_{u_0}^{\infty} w(u)\, \mathrm{d}u = 2\sqrt{\lambda/\pi}\, u_0 \exp(-\lambda u_0^2) + \operatorname{erfc}(\sqrt{\lambda}\, u_0). \tag{12}$$

We notice that Equation (12) depends only on $p = \sqrt{\lambda}\, u_0$. A molecule can only escape if (see Equation (1))

$$v_e = |\vec{v}_G + \vec{v}_M| \geqslant \sqrt{2}\, v_{\mathrm{K}}(R). \tag{13}$$

Because there are only few molecules which have a velocity of

$$u_0 = v_M \geqslant \sqrt{2}\, v_{\mathrm{K}}(R) - v_G \approx (\sqrt{2} - 1) v_{\mathrm{K}}(R), \tag{14}$$

only those molecules can escape whose velocity v_M is nearly parallel to $v_{\mathrm{K}}(R)$ (see Figure 2 and Equation (13)).

The average angular momentum of a molecule with mass $\tilde{m}$ is given by Equation (1):

$$C(R) = \tilde{m} v_G(R) R \approx \tilde{m} C_{\mathrm{K}}(R). \tag{15}$$

The average angular momentum of an escaped molecule is greater than the average molecular angular momentum of the gas by a factor of approximately $\sqrt{2}$. So the loss of angular momentum per escaped molecule is given by

$$\Delta C \approx 0.4 C_{\mathrm{K}}(R) \tilde{m}. \tag{16}$$

Due to the loss of angular momentum, the outer parts of the disk were shifted towards the central body. This is the starting mechanism for the main process.

5.2. The Formation of a Toroidal Gas Ring at the Edge of the Disk

The sum of forces which act on the gas in a unit volume must be zero: i.e.,

$$0 = K_G(R) = -\gamma M_c \varrho R^{-2} + \varrho v_G^2(R) R^{-1} - \operatorname{grad} p. \tag{17}$$

From this we obtain, for the angular momentum (cf. Equation (1)),

$$C_G(R) = (C_K^2(R) + \varrho^{-1}R^3 \operatorname{grad} p)^{0.5}. \tag{18}$$

The loss of angular momentum will inevitably cause R to decrease (grad p cannot change without a change of R and it is – at least initially – relatively small). But the gas falls into a region which already contains other gas. This causes the formation of a peripheral gas ring (see Figure 3).

In the outer part of the gas ring, grad $p < 0$ and, in the inner part, grad $p > 0$. In the centre ($R = R_K$ = Keplerian point; see Figure 3), grad $p = 0$. We approximate the velocity of the gas $v_G(R_K + r)$ near R_K by (see Figure 4; $C_A(R) = v_A(R)R$):

$$v_A(R_K + r) = v_K(R_K)/(1 + \zeta r/R) \approx v_G(R_K + r). \tag{19}$$

With this, the most important case in this theory, $\zeta = 1$ – i.e. $C_A(R_K + r) = \text{const.}$ – is obtained precisely. By substitution of (19) into (17) we get in a first-order approximation

$$\operatorname{grad} p = -(2\zeta - 1)\gamma\varrho M_c[r/(R + r)^3]. \tag{20}$$

By a comparison with (6) we see that we have the same force law for small r-values as we have for the vertical barometric equation. By integrating (20) we obtain the a radial barometric equation (cf. Equations (7a) and (7b)) with $T = \text{const.}$ (see Section 5.6) in the form

$$\varrho(r) = \varrho(0) \exp\{-(2\zeta - 1)\, 4.01 \times 10^{-15}\overline{m}(M_c/TR)(r/R + r))^2\}, \tag{21}$$

where $\zeta = 0.5$ corresponds to the limiting case $v_A(R) = v_K(R)$. For $\zeta = 1$, for small r-values we have the same pressure drop as in the vertical direction. With (7b) and (21), for $(r/R) < 0.1$ we can write

$$\varrho(r, h) = \varrho(0, 0) \exp\{-\eta_r(r/R)^2 - \eta_h(h/R)^2\}, \tag{22a}$$

where $\eta_h = 4.01 \times 10^{-15}\overline{m}M_c/(RT)$ and $\eta_r = (2\zeta - 1)\eta_h$; in the special case where $\zeta \approx 1$ we obtain, with $\eta = \sqrt{\eta_h\eta_r}$ and $d = (h^2 + r^2)^{0.5}$, a gas torus (see Figure 1)

$$\varrho(d) = \varrho(0) \exp\{-\eta(d/R)^2\}. \tag{22b}$$

If we set the condition that half of the gas torus mass is within the small radius r_T, then

$$r_T = \sqrt{\ln 2/\eta} \sim \sqrt{RT}. \tag{22c}$$

5.3. Generation of Shock Waves in the Gas Ring

During the shifting of the gas ring towards the central body the angular momentum increases on the inside and decreases on the outside as long as $C'(R) > 0$ according to (5a) and (5b). (Transport of angular momentum is negligible due to Section 4.4; see Figure 4.) But at that moment, when $C'_G(R) < 0$ for the outer parts of the ring, we get turbulence according to (5a) and (5b). When, owing to turbulence, the gas comes from the region outside the Keplerian point R_K (see Figure 4) towards the exterior

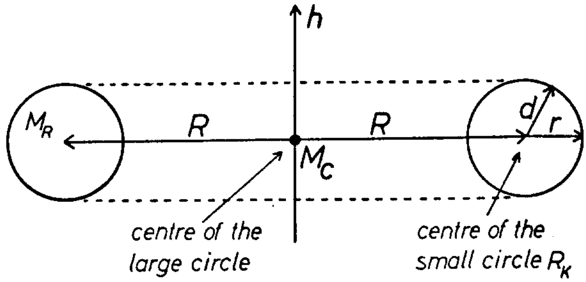

Fig. 1. Cross-section of the gas torus (or gas ring) with mass M_R.

regions of the ring, we have a big adiabatic expansion. The distance r_{SW} from the centre of the gas torus R_K, where the turbulence mainly causes the shock waves, is determined by the condition that grad p is at its maximum, i.e. $\partial^2 p/\partial r^2 = 0$. Because $p \sim \varrho$ we get, with (22a),

$$(r_{SW}/R_K) \approx (2\eta_r)^{-0.5} \approx 0.06. \tag{23}$$

The front of the expanding gas collides at high speed with the thin gas outside the ring (see Figure 5). We expect that the relative speed of this shock front is higher than the velocity of sound. This means there is an intensive heating and acceleration of the gas. The temperature T_{SW} generated by shock waves is approximately given by

$$T_{SW} = (\kappa - 1)p_1 T_1/(\kappa + 1)p_2, \tag{24}$$

where p_1 is the pressure and T_1 the temperature of the region from which the shock wave originates, and p_2 is the gas pressure through which the shock wave passes. The heated and accelerated gas is thrown out from the ring in a Kepler ellipse of high eccentricity. Some molecules can escape and thus reduce angular momentum. Others are ionized and we expect a plasma (see Section 5.8) in a state of partial corotation (A and A (1973); see Figure 3).

5.4. Energy balance of the contracting gas ring

Here we give a more precise analysis of the processes discussed in Sections 5.1, 5.2 and 5.3. In Figure 2, R is the great radius of the gas torus, and M_R its mass. The region where the gas diffuses out of the system has an average distance $\bar{r}_d$ from the centre of the small circle of the gas torus. Further, we denote the average angle between $\vec{v}_G(R + \bar{r}_d)$ and $\vec{v}_K(R + \bar{r}_d)$ by $\bar{\delta}$. The minimal thermal velocity $|\vec{u}_0|$ of the diffusing-off molecules is – according to (13) and the cosine law – given by (see Figure 2)

$$u_0^2 = 2v_K^2(R + \bar{r}_d) + v_G^2(R + \bar{r}_d) - 2v_K(R + \bar{r}_d)v_G(R + \bar{r}_d)\cos\bar{\beta}, \tag{25}$$

where $\bar{\beta}$ is the angle between $\vec{v}_G$ and $\vec{v}_K$. We assume that the Maxwellian velocity distribution is a good approximation for the distribution of velocities of the molecules

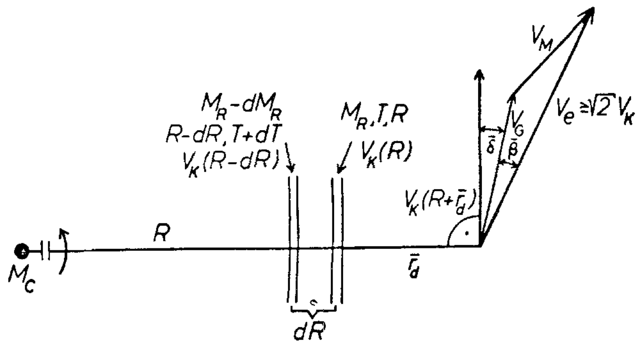

Fig. 2. Diffusing-off process of the molecules in the furthest out regions of the gas ring. Polar view. The great radius R of the gas ring with mass M_R is altered by dR if the gas mass dM_R has left the system. The molecules of the gas mass dM_R, which are diffusing off, have the thermal velocity v_M and the total velocity v_e. The region where this takes place is, on average, a distance $R + \bar{r}_d$ from the central body.

at the periphery of the gas ring. Then, for the mean values $\bar{v}_M$ and $\overline{v_M^2}$ of the diffusing molecules (using Equations (11) and (12)) we get

$$\overline{v_M^\nu} = \zeta_\nu u_0^\nu(\bar{\beta}) = \int_{u_0}^{\infty} u^\nu w(\lambda, u)\, \mathrm{d}u / N_0(\lambda, u_0); \qquad \nu = 1, 2. \tag{26}$$

We define, for simplicity, the mean total velocity $\bar{v}_e$ (see Equation (13) and Figure 2) of the diffusing-off molecules as

$$\bar{v}_e = \chi\sqrt{2}\, v_{\mathrm{K}}(R + \bar{r}_d). \tag{27}$$

According to the conservation law of angular momentum, the diffusion of the gas mass dM_R with the velocity $\bar{v}_e$ causes a reduction of R by dR. From Equations (1) and (27) we obtain (see Figure 2)

$$\begin{aligned} M_R C_{\mathrm{K}}(R) = {} & (M_R - \mathrm{d}M_R) C_{\mathrm{K}}(R - \mathrm{d}R) \\ & + \mathrm{d}M_R \chi\sqrt{2}\, C_{\mathrm{K}}(R + \bar{r}_d) \cos(\bar{\delta} + \bar{\beta}). \end{aligned} \tag{28}$$

With (1) one easily gets

$$\mathrm{d}M_R = 0.5[\chi\sqrt{2(1 + \bar{r}_d/R)} \cos(\bar{\delta} + \bar{\beta}) - 1]^{-1} M_R(\mathrm{d}R/R). \tag{29}$$

According to the virial theorem, through the reduction of R by dR we have an energy gain of

$$E_g = (0.5\gamma M_c/R) M_R(\mathrm{d}R/R). \tag{30}$$

The energy loss E_l due to the diffusing process of the gas mass dM_R can be obtained by two successive processes:

(1) Following the Virial Theorem, the energy necessary to transfer the gas mass dM_R from a circular orbit with a radius R and a velocity $v_{\mathrm{K}}(R)$ to a circular orbit with a radius $R + \bar{r}_d$ and a velocity $v_{\mathrm{K}}(R + \bar{r}_d)$.

(2) The energy necessary for gas diffusion to occur, i.e. that kinetic energy necessary to bring the mass of gas $\mathrm{d}M_R$ to a velocity $\sqrt{\overline{v_e^2}}$. With

$$\overline{v_e^2} = \xi \bar{v}_e^2 = \xi\chi^2 2v_K^2(R + \bar{r}_d), \tag{31}$$

and (27) we obtain, for the energy loss, the expression

$$\begin{aligned} E_l = {} & 0.5\gamma M_c \,\mathrm{d}M_R[R^{-1} - (R + \bar{r}_d)^{-1}] + \\ & + 0.5\,\mathrm{d}M_R(2\xi\chi^2 - 1)v_K^2(R + \bar{r}_d). \end{aligned} \tag{32}$$

By substituting $\mathrm{d}M_R$ from (29) into (32) the total energy balance E_G of the gas torus is given by

$$E_G = E_g - E_l = \left[0.5 - \frac{(\xi\chi^2 - 1)/(1 + x) + 0.5}{2(\chi\sqrt{2(1 + x)}\cos(\bar{\delta} + \bar{\beta}) - 1}\right]\frac{\gamma M_R M_c}{R}\frac{\mathrm{d}R}{R}, \tag{33}$$

where $x = \bar{r}_d/R$.

Next we would like to show that E_G is positive. This is necessary for the process to continue. For this we have to estimate $\bar{r}_d$. We can obtain a lower limit r_l for r_d via the following: The gas thrown out by turbulence and shock waves is first able to diffuse out where the mean free path λ_f of the molecules is in the order of $10^{-3}R$. It should be noticed that, due to the shock wave processes, the temperature in the outer regions of the gas ring is higher than in the centre. With $\zeta = 1.1$, $\bar{m} = 2.6$ and $(M_c/RT) \approx 1.05 \times 10^{16}$, and using Equations (21) and (22a), we obtain $\eta_r = 132$. Furthermore, we assume that the total mass M_R of the gas ring amounts to $0.02M_c$. Using volume integration of (22b), $\varrho(0)$ becomes

$$\varrho(0) = \eta(0.02M_c)/(2\pi^2R^3). \tag{34}$$

The mean free path λ_f is given by

$$\lambda_f = 1/(\sqrt{2}\,\pi\sigma^2 n) \overset{!}{=} 10^{-3}R, \tag{35}$$

where σ is the collision diameter with an estimated value of 2.5×10^{-10} m and n is the number of molecules per cubic metre; n is determined by (21) and (34). Combining (21), (34) and (35) gives us the lower limit r_l for the diffusing-off process

$$r_l/(R + r_l) = [\ln(8.6 \times 10^3 M_c/R^2)/132]^{0.5}. \tag{36}$$

We obtain the smallest value of all in the solar system for the orbit of Neptune, with $r_l/R = 0.65$. The average (r_l/R)-value for the solar system is about 0.75 and for the satellite systems about 0.9.

We must now consider the following. The gravitational contraction of the gas ring itself plays a big role for small r/R-values (see Section 6.1), yet its influence on r_l/R-values is insignificant. However, as the turbulence is essentially in the outer region, the $(\overline{r_l}/R)$-values are increased. Thus, we estimate that the average lower limit in the solar system for diffusing off is approximately $r_l/R \approx 0.9$. The mean value $\bar{r}_d/R$ is estimated to be 1.0.

We also need the values χ, $\bar{\beta}$, ξ and $\bar{\delta}$ for Equation (33). First, we calculate $v_G(R + \bar{r}_d) = v_G(2R)$ from (25). In order to do this we make the following plausible assumption: that gas which is thrown out due to turbulence and shock waves and which contributes to the diffusing-off process has an angular momentum of $1.15C_K(R)$. This gas moves in an elliptical orbit whereby its apogee is, on average, a distance $2R$ from the central body. This means that

$$v_G(2R) = 1.15C_K(R)/(2R) = 0.8132v_K(2R). \tag{37}$$

We assume further that where the gas diffuses, the angle between $\vec{v}_G$ and $\vec{v}_K$ is, on average, 4°. Assuming $u_0(\beta = 0) = 1.6 \times \sqrt{2kT/m_{H_2}}$ (see Equation (11)), and with (25) and (26) we obtain the following values by numerical integration: $\bar{\beta}(H_2) = 20.6°$ and $\bar{\beta}(He) = 15.2°$. With an average relative percentage by mass between H_2 and He of 1.1 we get $(\bar{\delta} + \bar{\beta}) = 24.3°$; further, we obtain with (26): $\zeta_1 = 1.179$ and $\zeta_2 = 1.190$. From this, and by Equations (25), (27), (31) and (37), we obtain $\chi = 1.0988$ and $\xi = 1.0113$. With (33) the energy gain is then given by

$$E_g = 0.196[\gamma M_c/R](dR/R) \sim R^{-1}. \tag{38}$$

For the upper limit of the energy gain we get a factor of 0.5 instead of 0.196, which means the energy gain is relatively large. As a lower limit for an energy gain one gets $x \approx 0.3$. Additionally, we have a relatively small energy gain due to the gravitational contraction of the gas ring itself.

5.5. Mean temperatures of the gas ring

The generated energy due to (36) is converted to:

(1) E_1 = thermal energy of the gas in the gas ring;
(2) E_2 = potential energy of the gas ring due to $|\text{grad}\, p| > 0$ and librational energy inside the gas ring;
(3) E_3 = heat radiation of the solid matter;
(4) E_4 = thermal radiation of the gas, which mainly consists of (a) radiation of the shock wave heated gas and (b) radiation of the plasma.

For high temperatures, i.e. $T > 400$ K, E_1 and E_2 are small in relation to E_3 and E_4. Thus E_3 and E_4, combined with (38), define the gas torus temperature for small R-values. According to the Stefan–Boltzmann law, the total radiated energy, S, in the period dt, for E_3 and E_4 is given by

$$dS/dt \sim AT^4 \sim R^2T^4, \tag{39}$$

where the torus surface $A = 4\pi^2 rR \sim R^2$. In the period dt, the energy loss due to radiation is proportional to the energy gain. If we now make the plausible assumption that for the relative contraction velocity v_c we have

$$v_c = dR/dt \sim R/M_R, \tag{40}$$

then it follows from Equation (38) that

$$\mathrm{d}S/\mathrm{d}t \approx \mathrm{d}E_G/\mathrm{d}t \sim (\gamma M_R M_c/R^2)(\mathrm{d}R/\mathrm{d}t) \sim \gamma M_c/R. \tag{41}$$

Combining (39) and (41) we obtain

$$T \sim R^{-0.75} \quad \text{for} \quad T > 400\ \mathrm{K}. \tag{42}$$

For large R-values one must note that after the cooling phase of the primeval hetegonic nebula, the gas in the outer region already has a temperature of about 35 K. Also, according to Equation (33), the gas in the gas ring warms up additionally, due to the main process. This means that RT is relatively higher. Then – since for large RT-values, χ, ξ and, above all, $\bar{\beta}$ are also high – the energy gain from (33) is considerably smaller than from (38). This is amplified by the fact that x is relatively small, as seen by (36). Thus, the temperature rise for large R-values is relatively small. For the solar system we estimate that

$$T = (0.7R + 900R^{-1})\ \mathrm{K}; \qquad R\,[\mathrm{AU}] > 2.2. \tag{43a}$$

On the other hand, for small R-values (<2.2 AU) we use Equation (42). However, according to Table II, the η-values are decreased as the R-values decrease. Furthermore, the contraction velocity is somewhat increased due to the expected dissociation of H_2 in the outer region of the gas ring, which has been heated by shock waves. So we substitute (42) with

$$T = (772R^{-0.80})\ \mathrm{K}; \qquad R\,[\mathrm{AU}] < 2.2. \tag{43b}$$

Thus, noting that solid matter, due to its loss of thermal energy, always has a lower temperature than gas (and a much lower temperature than plasma), we find the condensation temperature as a function of R closely agreeing with Cameron's (1975) and Lewis' (1973) temperature assumption (see also Section 5.10).

The thermal energy of the gas torus is generated by two processes:

(1) *By turbulence.* Because $C_G'(R) < 0$ there is a steady formation of thermal energy $\sim R^{-1}$ from Equation (5a).

(2) *By adiabatic compression.* The energy E_{ac} contained in one mole of gas, with volume V_0, in the gas torus is given by

$$E_{ac} = \int_{V_0}^{\infty} p\,\mathrm{d}V = (\kappa - 1)^{-1} p_0 V_0 = R_G T/(\kappa - 1) \sim T, \tag{44a}$$

where κ is the ratio of C_p to C_v. Because the generated energy due to (36) is $\sim R^{-1}$, it roughly holds that $E_{ac} \sim R^{-1} \sim T$. In the special case of a similarity transformation, $r/R =$ const., it holds that $T \sim R^{-1}$, $V \sim R^3$ and $p \sim R^{-4}$.

If there are adiabatic processes for a fixed R-value, the change of temperature is given by

$$T \sim V_0^{1-\kappa} \approx 1/\sqrt{V_0}. \tag{44b}$$

5.6. Transfer of Angular Momentum within the Gas Ring

For a contracting gas torus there are two mechanisms for a small transfer of angular momentum within the gas torus. During contraction new gas always moves from the gas disk into the gas torus, and a small amount of gas also shifts from the inner to the outer parts of the ring. With this (see Figures 3 and 4) we also have a slight transport of angular momentum. The second mechanism is caused by the shock wave processes in the outer parts of the gas torus and by turbulence: there is always a small radial displacement of the gas. From this we obtain a mixing of gas elements

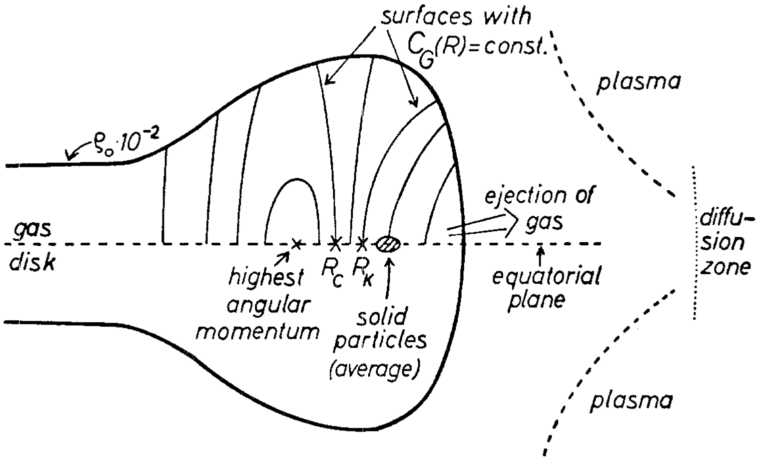

Fig. 3. Qualitative picture of the gas ring cut perpendicular to the equatorial plane. R_c is the centre of gravity of the small 'circle'. In the Keplerian point R_K we have the highest gas density ϱ_0. The plasma outside is in a state of partial corotation.

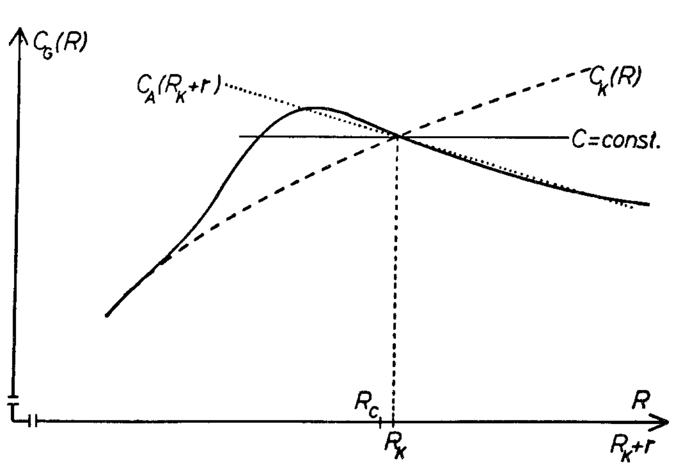

Fig. 4. Radial angular momentum distribution $C_G(R)$ of the gas within the equatorial plane of a non-librating gas ring. $C_A(R_K + r) = (R_K + r)v_A(R_K + r)$ is the approximate function of $C_G(R)$ in the neighbourhood of R_K (see Equation (19)).

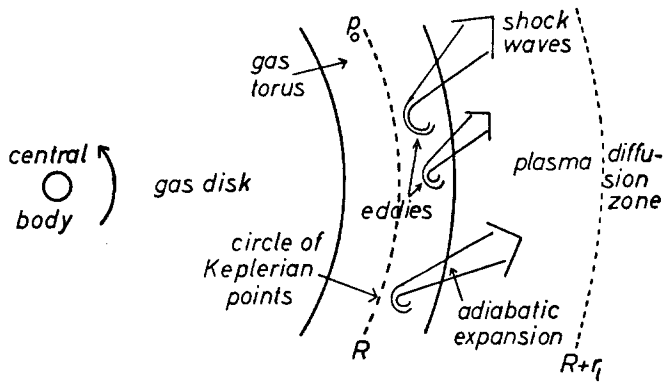

Fig. 5. Formation of shock waves induced by turbulence in the outer regions of the gas torus. Top view. The lower limit for the diffusing-off process is $R + r_l$ (cf. Equation (36)).

with different angular momenta, which causes a steady transport of angular momentum, generating new eddies. Outside the Keplerian point these eddies are the sources of new shock waves (see Figure 5). This second process can only take place if (see Equations (5a) and (5b)) $C'(R) < 0$ – i.e. with (19) and (21), $\zeta > 1$. For $\zeta \geqslant 1$ and small r/R values, we obtain as a measure of the intensity of turbulence in the gas torus using (5a), (5b) and (19)

$$W(R) = 2(\zeta - 1)v_{\mathrm{K}}^2(R) \sim R^{-1}. \tag{45}$$

Without angular momentum transfer, the difference between the angular momenta in the inner and outer parts of the gas torus, including ζ, would continually increase. On the other hand, according to (45) the intensity of turbulence, as well as the angular momentum transfer, is proportional to $(\zeta - 1)$ for $\zeta > 0$ and $\equiv 0$ for $\zeta \leqslant 1$. From this: (1) ζ must become greater than 1; and (2) we expect that ζ increases rapidly at first, but then there is only an asymptotic approach to an upper limit, which is conjectured to be 1.25.

5.7. Stability of the Gas Torus

Under 'stability', we understand first of all the stability of the middle part of the gas torus (region III in Figure 6) against large radial displacements. Three things are responsible for the stability of the gas torus:

I. *Dynamical Stabilization*

The gas torus is stabilized by the different angular velocity within the critical middle part of the gas torus because of $\omega(R) \sim R^{-\alpha}$ with $\alpha = \zeta + 1 \approx 2$. By this, all small local perturbations in the middle part are smoothed and balanced out. Because the shock waves are generated outside the middle part of the gas torus, its stability is not endangered.

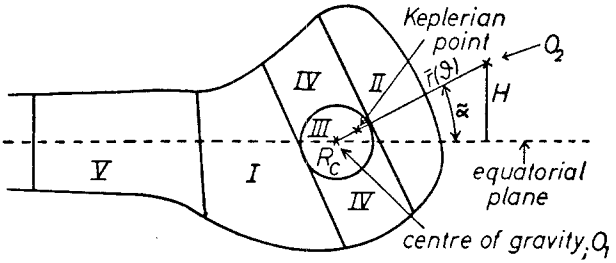

Fig. 6. Regions within the librating gas ring. R_c is the centre of libration. The angle between the two circular orbits O_1 and O_2 is α. H, $r(\vartheta)$ and $\bar{\alpha}$ are determined by Equations (50) and (51).

II. *Energetic Stabilization*

A radial displacement of the middle part with its great mass requires a great amount of energy. In order to bring the gas mass m_G from a circular Keplerian motion with a radius R to an elliptical Keplerian motion – with eccentricity ε – with the same angular momentum, one needs an energy $\Delta E(\varepsilon)$. This, with help of the vis-viva integral (see Glasstone (1965), chap. 2.54), is exactly given by

$$\Delta E(\varepsilon) = \tfrac{1}{2} m_G (\gamma M_c / R) \varepsilon^2 . \tag{46}$$

Radial displacements of gas masses $m_G \ll M_R$, such as those arising from turbulence, are, according to (46), always possible. However, large radial displacements of gas masses with m_R in the order of $10^{-3} M_R$, with $\varepsilon > 0.01$, cannot occur due to the dynamic stabilization of region III (see Figure 6) with its large gas mass. This is because we nearly always have an equilibrium of forces, so that the energy required in Equation (46) is not available. Further, we note that in region III of Figure 6, $\operatorname{grad} p \approx 0$.

But this is not true for the farther-out regions, since (1) here the effectiveness of dynamic stabilization decreases rapidly outwards; and (2) ϱ_G is relatively small and $\operatorname{grad} p \neq 0$.

III. *Thermal Stabilization*

According to Equation (22b), a radial or vertical displacement of a gas element inside the gas torus (see Figure 1) brings about an adiabatic compression or expansion. From (44b) it follows that

$$T \sim [\varrho(r, h)]^{\kappa - 1} . \tag{47}$$

This change of temperature is increased by the gravitational contraction due to the mass of the gas torus (see Section 6.1). Because of turbulence (see Section 5.5) such displacements always occur to a small extent for $\zeta > 1$, i.e. for a contracting gas ring.

Due to the repelling force, those gas elements which have a high specific weight (caused by high mean molecular weight and low temperature) are, on average, shifted to the centre of the gas ring. According to (39), the energy loss due to radiation varies approximately as T^4 – i.e. we expect the centre (region III) to be considerably cooler than with Equation (47). Also in region III (see Section 5.12) we find almost all solid matter with a high loss of energy due to radiation. Furthermore, there is a steady shifting of energy from the centre of the gas torus to its outer regions due to the shock waves.

Thus, as a good approximation we get $T =$ const.; we have already made this assumption in Equations (7a) and (21). But this means that the exchange of two gas elements located at very different distances from the centre, due to the repelling force, is only possible with a considerable expenditure of energy. This is evident because, according to Equation (47), the gas element shifted towards the centre has a lower gas density than its surrounding gas, while for the outward shifted gas element it is vice versa.

So we cannot determine the energy of this exchange process by using only Equations (5a) and (46). For $T =$ const. this exchange process is considerably hindered by (47). By this, the thermal stabilization hampers the fact that large radial displacements occur between regions II and III in Figure 6.

Since we expect no turbulence in regions V and I due to $\zeta < 1$ (see Figures 4 and 6; and Equation (45)), further stabilization of the gas ring is achieved.

5.8. Plasma in the outer parts of the gas ring

In the outer region (i.e. for $r/R > 0.2$ of the gas ring), plasma is produced by two processes. One possibility is the formation of plasma due to intensive heating of the gas caused by shock waves.

We assume that the central body rotates rapidly with regard to the gas ring and has a strong magnetic field. Then at least for small R-values the magnetic dipole field of the central body is sufficient to control the dynamics of a plasma. Since the total mass of the plasma is very small with regard to the central body's mass, then, according to A and A (1973), we expect the plasma to be in a state of partial corotation. As A and A have shown, the angular momentum C_{pl} of the plasma is given by the two-thirds law

$$C_{\mathrm{pl}}(R) = \sqrt{2/3}\, C_{\mathrm{K}}(R) \sim \sqrt{R}. \tag{48}$$

This means (ignoring grad p), that the R-value increases by a factor of 1.5 when the gas with an angular momentum $C_{\mathrm{K}}(R)$ becomes a plasma. By this one gets a large spatial separation between the centre of the gas ring and the plasma. Considering this spatial separation and the small plasma mass in relation to M_R, we rule out any disturbance of the gas ring by the plasma; this is also true if plasma instabilities, such as concentration into filaments, arise. The main process for the generation of plasma is as follows: The gas, accelerated by turbulence and shock waves, which runs into the region of the magnetized plasma has a high relative velocity compared to the plasma. The maximum relative velocities, v_r, are estimated (considering Equation (48)) to be of the order of $v_r \approx 0.5v_K$. By this all molecules with a mass m_K whose kinetic energy is larger than the ionization energy eV_{ion} are ionized: i.e.,

$$m_K \geqslant 2(eV_{ion})/v_{rel}^2 \sim R. \tag{49}$$

This is shown by Danielsson (1973) (see also references therein) and A and A (1974). As shown in Figure 3, we do not expect (at least for $(r/R) < 0.6$) a plasma in the equational plane because of the high number density according to (21) and (22a).

On the one hand there is a steady generation of plasma; on the other, a steady condensation of plasma. This condensation produces small grains, but this is only one source of solid matter formation.

The lower limit r_l for the diffusing-off process determined by Equation (36), is somewhat increased due to the plasma. If, say, $r/R > 0.7$, there is plasma, we expect a temporary and local disturbance of partial corotation when a large quantity of gas with high relative velocity with regard to the plasma penetrates its region. The consequences are local instabilities of the plasma, hydromagnetic shock waves, and formation of filaments. But here we are only interested in the transfer of the gas ring's angular momentum to infinity. Due to the plasma, and especially due to the occurrence of filaments, we estimate $\bar{r}_d/R \approx 1.2$. Further, we note that if there is plasma in the far outside regions of the gas ring, the Maxwellian velocity distribution is only a very rough approximation. That means that if there is plasma, the transfer of angular momentum to infinity is somewhat more effective than according to Section 5.4. The total mechanism is analogous to that in the solar corona; instead of the solar wind we have a 'torus wind'.

The total process proceeds as follows: There is an energy transfer from the centre of the gas torus to its outer regions. Dissipation of the light elements causes a loss of angular momentum. According to (33) this produces an energy gain. Which particular process occurs, depends essentially on the distance from the central body. In the vicinity of the Sun the mechanism for the generation of the torus wind is nearly identical with that for the solar wind, but for large R-values one has only the dissipation of neutral H_2 and He as shown in Section 5.4.

5.9. Building-up process of a libration within the gas torus

During contraction there is another important process. The inner and outer parts of the ring begin to swing around the centre of gravity $R_c \approx R_K$ (see Figure 6). There is only one way for this building up of a libration to be able to take place. All the gas which has the same position within the gas torus (i.e. the same distance R from the central body) rotates within the same plane. The gas in the inner part and the gas in the outer part of the torus rotate in planes which are inclined against each other. All other librations within the ring are neutralized by interference caused by the dynamical stabilization (see Section 5.7).

In a first-order approximation we can assume that all gas elements move in circular orbits. We are now only considering those gas elements whose centre of their circular orbits coincides with the central body; only these gas elements pass the line $r(\vartheta)$ (see Figure 6).

We take as a reference circle O_1 the circular orbit with radius R_c of the gravity centres of the gas torus' small circle. Further, we take a circle O_2 with radius $R_c + r_0$. The angle between O_1 and O_2 we denote by α. As a reference point we take a gas element GE_1 on the reference circle O_1 with the angular velocity $\omega_K(R_c)$. The distance $r(\vartheta)$ (see Figure 6) between this gas element GE_1 and the circle O_2 is then, for $\alpha < 10°$, in a good approximation given by

$$r(\vartheta) = [r_0^2 + R_c(R_c + r_0)\sin^2\alpha\sin^2\vartheta]^{0.5}; \qquad \vartheta = \omega_K(R_c)t. \tag{50}$$

The orbits of all other gas elements move on circles which have the same line of intersection with the reference circle O_1 as circle O_2; further, these circles cut the section $r(\vartheta)$. For the distance between the orbiting reference point GE_1 and one of these circles we have $yr(\vartheta)$, with $y = \text{const}$.

We denote the centre of gravity along the line $yr(\vartheta)$ with $y \in [0, \infty]$ as $\bar{r}(\vartheta)$. So the sinusoidal libration of the gas outside R_c out of the plane of O_1 around GE_1 can be described (see Figure 6) as

$$H(R_c, \alpha, \vartheta) = [R_c + \bar{r}(0)]\sin\alpha\sin\vartheta; \qquad \vartheta = \omega_K(R_c)t. \tag{51}$$

The angle $\tilde{\alpha}$ in Figure 6 is determined by the cosine law: $(R_c + \bar{r}(0))^2 = R_C^2 + \bar{r}^2(\vartheta) - 2R_c\bar{r}(\vartheta)\cos\tilde{\alpha}$. The same holds, of course, for the gas inside R_c but here we have to substitute ϑ by $\vartheta - 180°$.

Let us assume that there is already a small libration. Then the loss of angular momentum per period $C'(t)$ is not monotonous but is coupled to the libration (51) of the torus. Maximum loss of angular momentum occurs when the outer and inner parts of the ring are passing the plane of O_1, i.e. if $\vartheta = 0$ in Equations (50) and (51). Since $r(\vartheta)$, according to (50), for $\vartheta = 0, \pi$ attains the minimum value, and we get an adiabatic expansion when the inner and outer parts of the gas ring are moving out of the plane of O_1. The volume of any gas element $\sim r(\vartheta)$; with (44b) it follows that

$$T \sim r^{1-\kappa}(\vartheta); \qquad p \sim r^{-\kappa}(\vartheta). \tag{52}$$

We denote by $X = yr(\vartheta)$ the distance of a point on the section $r(\vartheta)$ from circle O_1. Due to the conservation law of angular momentum, the partial derivative of the angular momentum $C_G(X, \vartheta)$ in the direction $r(\vartheta)$ is

$$\frac{\partial}{\partial X}C_G(X, \vartheta) = (r(0)/r(\vartheta)) * \frac{\partial}{\partial X}C_G(X, 0). \tag{53}$$

In every other direction C'_G is smaller. According to (45) and (53) we get, for the intensity of turbulence,

$$W(R_c, \vartheta) = 2(\zeta - 1)v_K^2(R_c)(r(0)/r(\vartheta)). \tag{54}$$

Summarizing, we can say that for the zero passage of this libration: (1) we have the highest intensity of turbulence and (2) T, p and grad p have then their highest values – which means that, according to (24), we have also the maximal values for p_2/p_1 and

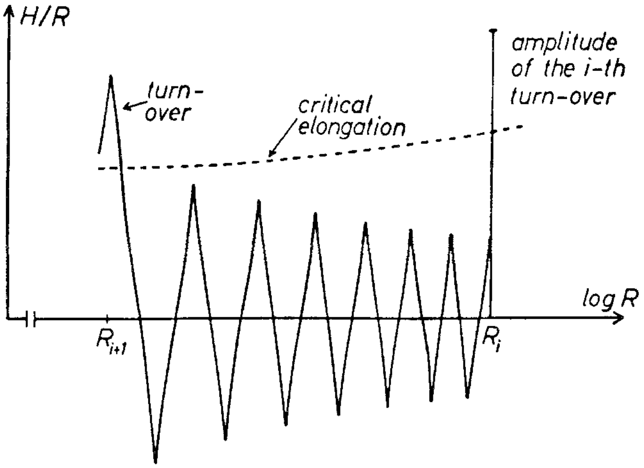

Fig. 7. Motion of the outer part of the gas ring (more precisely, of the point O_2 in Figure 6) in a corotating relative system between two consecutive turn-over processes. H is (see Equation (51)) the elongation out of the central plane. The turn-over process occurs when the critical elongation is reached. When the gas ring contracts again, a fixed portion of the amplitude of the turn-over always remains.

T_1 and $T_{SW} \sim [r(0)/r(\vartheta)]^{2\kappa-1}$. So we have the highest loss of angular momentum during the zero passage.

By this the outer part of the gas ring is moving on inclined planes towards the central body when it goes through its zero position; the situation for the inner part of the gas torus (where the amplitude is somewhat smaller) is equivalent to a mathematical pendulum whose thred is shortened when it is passing through its zero position.

In both cases we get an increase in libration amplitude $H(R_c, \alpha, 90°)$ (see Equation (51)). This building-up process of the libration as a function of R_c is shown in Figure 7.

5.10. Turn-over process

As long as the angular momentum of the gas in the inner part (region I) is smaller than in the outer part (region II) of the ring – according to Equations (5) and (45), with $\zeta < 1$ – an exchange, of course, would need energy (cf. Figure 6). If the distribution of angular momentum is the other way around, then, in principle, this process could take place with a gain of energy (Equation (45), with $\zeta > 1$). This means that we would have a metastable situation. But in our situation region III, which is in the middle of the gas ring and has the highest gas density, is situated between them. A shifting of region III needs a great amount of energy and the forces which act upon this region compensate each other. Therefore, this region will not change its position. Thus, an exchange of the inner and outer parts of the ring can take place only by a rotation around region III (see Figure 6). But such a turn-over process requires a great amount of energy because it leads to a notable change in the orbits of the gas within the inner and outer parts of the ring; also, the orbits of region IV have to be changed. Therefore, since ζ is always relatively small ($\leqslant 1.25$), one needs a building-up process of a libration as described in Section 5.9 for the turn-over process to occur (see Figure 7). When, according to (51) and (22c), the libration has reached the critical height, H_c with

$$H_c(R_c, \alpha_c, \vartheta = 90°) \approx R_c\sqrt{\ln 2/\eta}, \tag{55}$$

the turn-over process takes place at one of the two points $\vartheta = 90°$ or $270°$ in (50) and (51) where the displacement of the equilibrium position of the libration within the gas ring has its maximum. The point of turn-over is fixed in space and the turn-over process takes place during one orbital period of the main part of the gas ring. During the turn-over process there is a considerable adiabatic expansion of the gas within the gas ring.

First, let us consider the special case of a non-librating gas torus ($\alpha = 0$ in Equations (50) and (51)). Let ζ_b and ζ_a denote, respectively, the coefficient in Equation (19) for the radial velocity distribution before and after the turn-over process. Using the conservation law of angular momentum we obtain, with (22a),

$$\zeta_a = 1 + u - \sqrt{u(1 + u)}; \qquad u = (\zeta_b - 1)^2 T_a/(2\zeta_b - 1)T_b, \tag{56}$$

where T_b is the average temperature before, and T_a the average temperature after the turn-over process. According to (44b) and (22a), by adiabatic expansion we obtain $T_a/T_b = [(2\zeta_a - 1)/(2\zeta_b - 1)]^w$, with $w = (\kappa - 1)/(\kappa + 1)$; from this, and with $\xi_b = 1.25$ and $\kappa = 1.5$, we get $\zeta_a = 0.844$ and $T_a/T_b = 0.85$.

For the librating gas ring we can only establish an average value for the temperature in relation to ϑ, using (50) and (52). Before the turn-over process, with $\alpha \approx 3°$, we get $\bar{T}_b \approx 0.89 T_b(\vartheta = 0°)$. After the turn-over process, with $\alpha \approx 5°$, we get $\bar{T}_a = 0.85 T_a(\vartheta = 0°)$. Therefore, due to adiabatic expansion we can approximate the total average temperature decrease with $\bar{T}_a/\bar{T}_b \approx 0.81$.

The gas ring is already asymmetrical before the turn-over process, especially due to the gas disk adjacent to its inside. According to Equation (5a), only those inner gas regions where $C_G(R) > C_K(R_c)$ can take part in the turn-over process, and from Figures 4 and 6 we see that this is true for region V. Further, we expect that the ζ-value for the outer torus regions is somewhat greater than that for the inner regions. Therefore, it is conjectured that $R_c < R_K$ (see Figure 4). By this a turn-over of region III is at least partially hindered. Moreover, as a consequence, region II has a greater libration amplitude than region I.

During the turn-over process regions I and II slide over region IV, but they themselves do not turn over. From this we get an angular momentum distribution as seen in Figure 8a, with a somewhat larger $\bar{\zeta}_a$-value than according to Equation (5b); we estimate that $\bar{\zeta}_a \approx 0.9$.

According to Figure 8a, we get two librating gas rings with opposition of phase and a period of libration of $2\pi\omega_K(R)$. The centres of these rings, R_s and R_p, are defined by $C_G(R) = C_K(R)$, or, similarly, by grad $p(R) = 0$. The vectors in Figure 8a qualitatively show the amplitude of oscillation for different R-values.

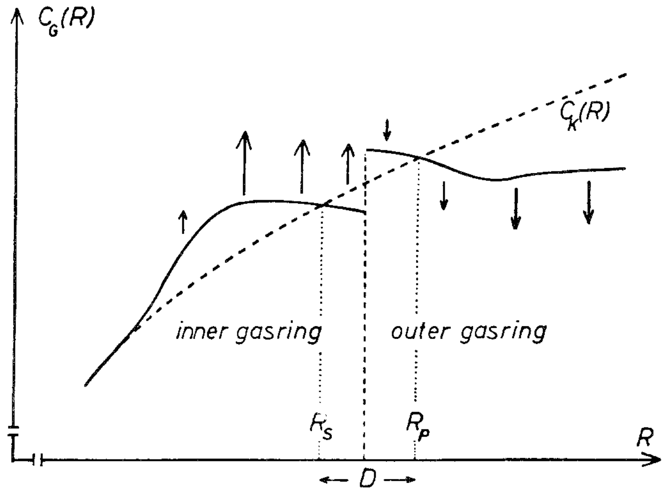

Fig. 8a. Angular momentum distribution of the gas immediately after the turn-over process. R_s and R_p are the great radii of the inner and outer gas rings. The vectors show qualitatively the amplitudes of oscillation for different R-values.

By the turnover process not only the vertical (in relation to the central plane) oscillation energy is increased. The energy present according to Equation (5a) is also converted into radial oscillation energy. We estimate the inclination of the centre of the inner ring with radius R_s to the central plane to be, on average, 5° and that of the outer ring with radius R_p to be 2°. These values, however, are dependent upon the r/R-values $\sim 1/\sqrt{\eta}$ according to (22c) and (43) (see, moreover, Section 6.1 and Table II).

5.11. Recommencement of the contraction

After turn-over the speed of contraction is drastically reduced because of $\bar{\zeta} \approx 0.9 < 1$, due to Equation (45). From the distribution of angular momentum in Figure 8a we see that there is a region with $\zeta > 1$ not only in the outer gas ring but also in the inner gas ring, which means there is turbulence. But since $(\zeta - 1)$ is very small and, moreover, because temperature and pressure are reduced by the turn-over process, the loss of angular momentum according to Sections 5.3 and 5.4 is relatively small.

Owing to the reduced speed of contraction and the energy loss by radiation, the temperature in the outer parts of the outer gas ring decreases more and more. Also, the plasma condenses out. But this does not hold for the outer part of the inner gas ring. We have, namely, a very large energy reservoir consisting of the radial and vertical oscillation energy. On the border between the inner and outer gas rings most of this energy reservoir is slowly transformed into thermal energy, owing to the strong turbulence present. This happens essentially only for those two places where the planes of the inner and outer gas rings intersect. Only here do we have high pressure and high temperature; therefore the total loss of energy due to radiation is relatively small.

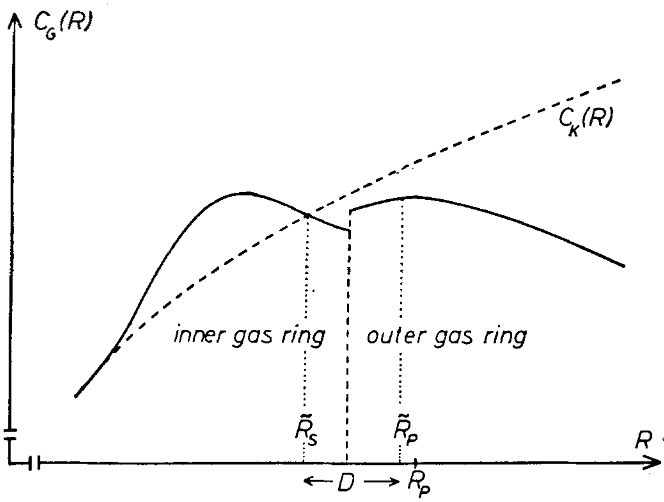

Fig. 8b. Angular momentum distribution of the gas immediately before the recommencement of contraction. The inner gas ring has already partially absorbed the outer gas ring.

Shock waves generated in these two regions move into the relatively cool and low-density gas (due to the inclination between the two gas rings) of the outer gas ring. According to Section 5.4, the energy gain due to the high $\bar{X} = \bar{r}_d/R$-value is larger than that according to Equation (38).

The gas mass of the outer gas ring is slowly absorbed by the inner gas ring due to dissipation processes and because a large part of the low angular momentum ejected gas of the inner gas ring is captured by the outer gas ring. An in-between situation can be seen in Figure 8b. Although here the gas mass of the outer gas ring has already been largely absorbed by the inner gas ring, the centre of the outer gas ring has only been slightly displaced from R_s to $\tilde{R}_s$.

Together with the reduction of the gas ring there is an increase in the total average $\bar{\zeta}$-value and in the speed of contraction. Finally, from the turn-over process there remains only a small but important share of the vertical libration energy (see Figure 7).

5.12. The formation of two rings of matter

According to Equations (1), (3) and (19) there is in the gas ring a relative velocity $v_{\text{rel}}(R, r) = v_{\text{K}}(R)(\zeta - 0.5)(r/R)$ between the gas and the solid particles. This brings about a frictional force f. At least for the larger grains (= planetesimals) – for which we assume there to be spheres with radius r_p, mass m_p and density ϱ_p – this force f can be written as

$$f(r_p, r) = c_f \pi r_p^2 \varrho_g(R, r) v_{\text{rel}}^2, \tag{57}$$

where c_f is in the magnitude of 0.1, and $\varrho_g(R, r)$ is the gas density from Equation (21). The acceleration b_f of the planetesimals is given by f/m_p. With $X = r/R$, and from

Equations (21) and (57), we get

$$b_f(R, r_p, x) = 0.75c_f(\zeta - 0.5)^2(\varrho_p r_p)^{-1}v_K^2(R)\varrho_g(R, 0)X^2 \exp(-\eta_r X^2). \quad (58)$$

Owing to this all solid matter outside R_K is continuously decelerated. This means that when the large radius of the gas torus has been reduced from one turn-over with R_i to the next turn-over with R_{i+1}, all condensed matter which was within this region is also shifted (with a small retardation) towards the central body and remains inside the gas torus (see Figures 3 and 9).

There is, however, an upper limit to the radius $\hat{r}_p$ of the shifted planetesimals, but this only plays a role for the solar system with large R-values: for $R = 30$ AU, $\hat{r}_p$ is in the region of 10 m; for $R = 50$ AU it is only about 0.1 m. It can be assumed that this is one source for trans-Pluto matter.

Without turbulence we get, according to (58), as a consequence of $b_f \sim r_p^{-1}$ a spatial separation with respect to the size of the solid bodies: small grains are near the Keplerian point R_K, the planetesimals are farther away. Due to turbulence in this region, this distribution holds only on average. Figure 3 points out the region where we expect to find most of the solid particles. The greater particles move on slightly eccentric orbits, which is mainly caused by turbulence, but which also is due to the circumstance that many particles are condensed out of the plasma (for which the two-thirds law holds – cf. (48)). Through this the larger particles are able to accumulate continuously, leading to the formation of planetesimals. But with the increasing mass of the planetesimals the accumulation speed decreases because, according to (58), the r-values get too large.

Further, for $\zeta > 1$ the inner and outer parts of the gas torus apply a torque on each other, which results in a precession of the inner and outer parts of the gas ring. The solid bodies partake in this precession with a retardation due to friction (see Equation (57)). The greater the solid bodies, the greater the inclination between their orbits and that of the outer parts of the gas ring. (This also decreases the accumulation speed of the greater planetesimals.) This is the first step in the formation of a jet stream.

Before the turn-over process takes place, we only have one ring of solid matter.

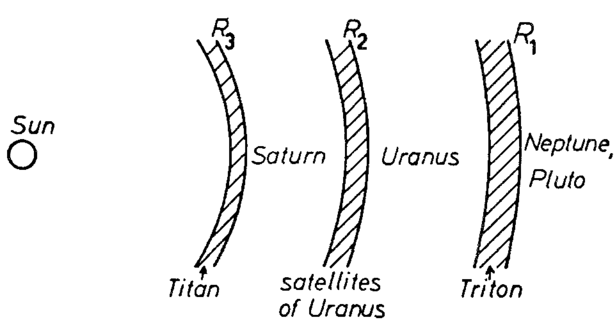

Fig. 9. Quantitative picture of those regions out of which the matter of the planets and of their satellites originates.

Due to the adiabatic expansion caused by the turn-over process the temperature of the gas decreases roughly by a factor of 0.8 (see Section 5.10). Accordingly, a part of the gas in the inner ring (see Section 5.10) can condense. Furthermore, according to Equation (58) and because $b_f \sim (r_{\text{pl}}\varrho_{\text{pl}})^{-1}$, with the turn-over process small and lightweight grains are transported to the inner regions. This is also solely effective for small R-values, because $\varrho_0 \sim R^{-3}$ holds in a good approximation. This is the main source of solid matter in the innermost (adjacent) ring of matter near the Sun (especially for Mercury and the Moon). A second source of solid matter comes from the outermost region of the gas disk adjacent to the gas torus (see region V in Figure 6 and the hatched regions in Figure 9). The outer part of the gas torus (region II in Figure 6) falls into this region due to the turn-over process, and all the solid matter that was within this region is collected by the inner gas ring. This is more favourable for large R-values, since here the small radius r_T of the gas torus – see Equations (22c), (43a), (43b), Section 6.1 and Table II – is greater in relation to R. So we get the two inclined adjoining rings of matter. The mass ratio of the two rings of solid matter is in the order of 1:100.

5.13. Accretion of Planets from the Outer Matter Band

For the component of the angular momentum of the gas ring perpendicular to the original gas disk $C_\perp(R)$ one gets

$$C_\perp(R, \bar{\alpha}) = M_R\sqrt{\gamma M_c}[\sqrt{R}\cos\bar{\alpha}]. \tag{59}$$

Accordingly, $\bar{\alpha}$ is the average value of $|\alpha|$, where α is the inclination angle of the gas elements within the gas torus. By the turn-over process $\bar{\alpha}$ increases by about 2° and, therefore, as a result of the conservation law of angular momentum, R according to (59) also increases, which means that the gas of the gas ring is, on average, shifted to a slightly higher orbit.

For the formation of planets there are four intermediate phases:

I. Dust and grains (formed mainly by condensation from the initially hot hetegonic nebula, but also by condensation from the plasma outside the gas torus) are collected within the gas torus by the contraction process; the first planetesimals were also formed by this method.

II. This is the most essential intermediate phase. By the turn-over process the outer gas ring (that is, the original inner parts of the gas ring) takes on a higher orbit (see Figure 10). This effect is reinforced according to Equation (59). By this the orbital period ($\sim R^{1.5}$) is reduced. Because the turn-over process lasts for one orbital period of the centre of the original gas torus, we get a gap in the outer gas ring (see Figure 10). This gap is present for a few orbital periods. Gravitational forces are now operating from the gap into the gas ring (see Figure 10) which accelerate the dust and the grains tangentially away from the gap. If the quantity of solid matter is sufficient, this leads to the *formation of two proto-planets*, which usually capture each other fairly quickly.

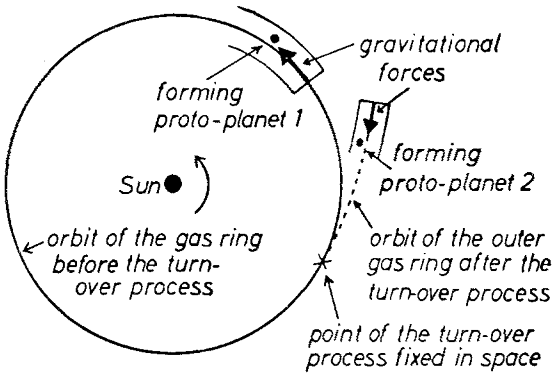

Fig. 10. Formation of the two proto-planets in the outer gas ring immediately after the turn-over process.

III. Owing to the asymmetry of the original gas ring ($R_c < R_K$, see Figure 4) its middle part is shifted somewhat upwards. Hereby, with Equation (59), and due to friction with the gas (Equation (58)), the grains are shifted into the region of the planetesimals ($\approx R_p$ in Figure 8a). Furthermore, turbulence, contraction speed and the precession of the outer gas ring are all drastically reduced. Therefore, not only the proto-planet but also the planetesimals grow very quickly.

IV. The growing proto planet (embryo) disturbs the orbits of the planetesimals (and also there is a perturbation of the planetesimals between each other), which means a *jet stream* is formed and the ε-values of their orbits increase. By this the perigee of these orbits comes nearer to the central body. Owing to friction and the collection of grains, the a-values as well as the inclination angle of the planetesimals' orbits to the central plane decrease. For large planets the perigee of these planetesimals is within the gas disk inside the inner gas ring, and these planetesimals sweep up the grains of this region at a rapid rate.

Because the orbital period is $\sim a^{1.5}$ we get an increasing difference between the angular velocity of these planetesimals and the growing planet. The accretion process is further promoted by the fact that the growing planet is moving within the outer gas ring. This means it is surrounded by a very dense and vast atmosphere. Thereby its mass is enlarged as well as the capture cross-section. Most of the planetesimals which run into this atmosphere are either vaporized or captured due to a slowing-down caused by great friction often reinforced by the dispersion of the planetesimals.

As Giuli (1968a, b) has shown, the rotation of planets will be prograde if accretion takes place from eccentric orbits. Qualitatively, this is transferable to this theory. But Giuli's (1968b) quantitative results do not apply here because: (1) he has assumed equal grain density in different orbits; (2) he has omitted the friction between the planetesimals (grains) and the gas, especially in the vast dense atmosphere of the accreting planets; (3) he has assumed that the particles move in the same plane as the planet; and (4) we also have to take into account in this theory the gravitational influence of the gas ring.

We expect a slightly higher spin C_{sp} of the planets than Giuli (1968b) has calculated, because we have an accretion from two jet streams with heliocentric orbital elements $a < R_0$ and $\bar{\varepsilon} \approx 0.02$ and, further, an accretion mainly caused by the hot, extensive atmosphere ($C_{\text{sp}} \sim \sqrt{r_p}$, where r_p is the perigee of the infalling bodies). These two jet streams have the same average a- and ε-values and have also the same inclination to the growing planets' orbit (about 1.5°), but where the one jet stream has its apogee the other has its perigee. (As A and A (1970b) have shown, the optimal orbital data for the jet stream forming the Earth are: $a = 0.96$ AU and $e = 0.03$.) But for a quantitative analysis of the spin coming from the collection of the jet stream associated with the outer gas ring one needs further clarification (see also Sections 5.15 and 6.3).

The energy one gets by the accretion process is very large. If the density ϱ_p is constant for the final planet with mass M_p and radius R_p, one easily gets for its formation energy the expression

$$E_{ac} = 0.8\pi\varrho_p R_p^2 M_p . \tag{60}$$

Because the gas in the outer gas ring is optically thin, a great amount of E_{ac} is radiated off. Another very effective mechanism for the removal of E_{ac} is as follows: when the gas pressure of the outer gas ring vanishes (due to the recommencement of the contraction), we get a large decrease in the atmospheric mass of the planet, which considerably reduces the energy according to Equation (60).

The accretion time for the planets and satellites is significantly shorter than in almost all other theories.

5.14. Development of the Matter Band Belonging to the Inner Gas Ring

Analogous to the process which leads to the gap in the outer gas ring (see Section 5.13 and Figure 10) we have, for the inner gas ring, an overlapping region which is (according to Equation (59)) a little bit smaller than the gap of the outer gas ring. Thus, gravitational forces are directed into this overlapping region. If there is enough solid matter in this ring, a larger body can be formed.

Further development now only depends on how quickly the planetary accretion in the outer gas ring takes place. We assume that the minimal distance D between the centre of the two gas rings, $D = R_p - R_s$ in Figure 8a, is constant, which also means that, later, $\tilde{R}_p - \tilde{R}_s = D$ in Figure 8b, where R_p and later $\tilde{R}_p$ are the distances between the accreting planet and the central body.

With increasing mass and constant D there are three successive phases for the development of the inner jet stream:

I. Because the mass of the accreting planet is too small, it is impossible for it to collect the matter of the inner jet stream.

II. The jet stream is captured in a retrograde direction, which corresponds to the trajectory 90.9 in Dole's paper (1962).

III. The jet stream is captured in a prograde direction, corresponding to the trajectory 91.2 in Dole's paper (1962).

One point is very important. Not only is condensed matter captured, but also the gas from the region slightly outside the centre of the inner gas ring (see Figure 8b). This capture from a circular orbit is favoured because of the low angular velocity (see Equation (19)) of this gas (which means that the difference between the angular velocities of this gas and of the planet are relatively small) and as a result of the ejection of gas due to turbulence and shock waves. But this cannot take place until the density of the gas surrounding the planet (that is, outside its atmosphere) is lower than the gas density of that region from which the gas comes. Then, the inclination angle between the orbit of the planet and the centre of the inner ring has also decreased (to about 3°).

If there are greater planetesimals, their capture is relatively independent of the capture of the gas. Because the mass of the gas is greater by a factor of 10^2 than that of the condensed matter, the capture of this gas into a circumplanetary disk has the most important influence on the spin period and on the inclination of the equator to the orbit of the planet.

Owing to friction, and because the gas is captured in a wide stream, one does not have the diversity of trajectories as calculated by Dole (1962) but only a prograde or retrograde capture.

The formation of an 'accompanying planet' (like Triton) in the inner gas ring is only possible if there is enough mass and if, at the end of the planet formation (which is given by the beginning contraction of the inner gas ring), the planet has just started with the retrograde capture of the gas and solid bodies (phase II, above).

A summary of all processes and consequences of the capture of matter from the inner gas ring is given in Table I. A quantitative analysis for this is given in Section 6.

5.15. Spin and inclination of equator to orbit of the planets

If the mass ratio between the greatest planetesimals and the planet is small – such as in this theory – and if the complete system is always plane, there is no inclination of equator to orbit. Marcus (1967) and Safronov and Zvjagina (1969) have shown that within their planetesimal concept the above mass ratio is so great that a statistical distribution of the inclination of equator to orbit seems possible. But if one looks at the inclination angles of the 'regular' planets, one sees that there is no statistical distribution. In this theory the planets were formed from matter which orbits in different planes. The planetary spin vector has two components:

(i) $\vec{S}_o$, which is the result of the planet collecting matter from the outer jet stream in a prograde direction. The planet collects the planetesimals as well as dust and gas from the outer jet stream. We expect a small inclination of equator to orbit and, for the sake of simplicity, we take here 0°.

TABLE I

Consequences of the capture process of gas and solid matter from the inner gas ring caused by the planets

Planet	Process	Most important consequences
Venus	No capture of matter; 'inverse swing-by process'	Small spin; no satellite; Mercury and its orbit
Earth	Prograde capture	Moon
Mars	Retrograde capture of a small quantity of matter	Relatively small spin; Asteroid Pallas
Jupiter	Prograde capture	Regular satellites
Saturn	Prograde capture	Regular satellites; especially Titan
Uranus	Retrograde capture	Spin axis of 98°; relatively small spin; regular satellites
Neptune	Retrograde capture of a small quantity of matter [Swing-by process]	Relatively small spin; Triton; [Pluto = proto-planet 1; see Section 5.13]

(ii) $\vec{S}_i$, which is a result of the capture of matter by the planet from the inner gas ring in a retrograde or prograde direction, depending on ΔR and the final mass of the planet M_p; we expect an inclination of equator to orbit of about 145° and $-35°$, respectively.

Therefore, it is essential that $\vec{S}_o$ and $\vec{S}_i$, due to the inclination of the two rings to each other, are never anti-parallel.

Most of the spin $\vec{S}_o$ is contained in the huge oblate spherical atmosphere. Because of the friction between the gas in the outer gas ring and the planet, due to their relative velocity, one expects only a small gas disk outside the huge atmosphere. The captured gas from the inner gas ring also travels into the planet's atmosphere when it forms the circumplanetary disk. Owing to turbulence and high temperatures (one expects a very thick gas disk and plasma) one gets one system (including planet, atmosphere and gas disk) with a spin vector $\vec{S}$ given by the addition of $\vec{S}_o$ and $\vec{S}_i$.

We assume that the mass of the gas disk is about 5% of M_p, the average distance from the centre of the planet with radius R_p is about $20R_p$; the angular velocity ω_p of the planet just formed and of its atmosphere is about $0.03\omega_K(R_p)$, and the angular momentum of the planet together with its atmosphere is about $2M_pR_p^2\omega_p$. So we find that the angular momenta S_{pa} (= spin of the planet and its atmosphere) and S_d (= spin of the gas disk) have the same order of magnitude. Normally it holds that S_d is greater than S_o by roughly a factor of 4.

The final planetary spin S_p is the sum of S_{pa} and of the angular momentum S_r which the gas ring has when it is absorbed (after many turn-over processes) by the outer regions of the planet's atmosphere.

5.16. Differences between the Planetary System and the Satellite Systems

According to the hetegonic principle, the formation process of the satellite systems is the same as for the planetary system. In spite of this there are, however, four differences between the two formation processes:

(a) Because the angular velocities of the planets just accreted are relatively low, one does not expect an extensive transport of angular momentum from the central body to the gas disk – as assumed in the solar system (see Section 3); this means there is no separation between atmosphere and gas disk.

(b) At the end of the main process the gas ring is absorbed by the central body. The additional angular velocity which the central body gets due to this is smaller by at least a factor of 10 for the Sun (see Section 6.2) than for the planets.

(c) The acceleration of the solid matter due to friction with the gas within the circumplanetary disk is (according to Equations (57) and (58)), on average, greater by a factor of 10^5 than in the circumsolar disk.

(d) The main process for the satellite systems is influenced by the gravitational field of the Sun. As a consequence of the great gravitational quadrupole moment of the system consisting of the oblate planet and atmosphere and the gas disk, this system precesses, perturbed by the Sun, with the same angular velocity. However, this is not true for the gas ejected far away from the outer regions of the gas ring with an apogee near the Lagrangian radius of the planet. It has a higher precessional rate and by this the building of a libration is hastened. Therefore, the average R_{i+1}/R_i-values are smaller for the satellite systems with respect to the solar system.

A more detailed analysis of (b), (c) and especially of (d) will be given in Part II.

6. First Applications of the Theory

6.1. Calculation of the Small Diameters of the Gas Tori

Owing to the contraction without new gas coming in from the gas disk, we have a mass loss – cf. Equation (29). Since, normally, there is a plasma in the state of partial corotation outside at the gas torus (cf. Section 5.8), in Equation (29) we take the following values into account: $\overline{r_d}/R = 1.2$; $\chi = 1.15$ and $(\bar{\delta} + \bar{\beta}) \approx 30°$. By integration of (29) for the mass M_R of the gas ring contracted from R_0 to R we get

$$M_R(R/R_0) = M_R(1)(R/R_0)^{0.46}. \tag{61}$$

For the calculation of the $\bar{m}$-values (see Equations (7), (21) and (22)) we take the abundances of elements estimated by Urey (1972). For the atomic abundances we have 90.752% H-atoms, 9.075% He-atoms and 0.173% atoms of other elements; for the percentage ratio by mass we get 69.9% H_2, 27.9% He and 2.2% for all other elements. Since the torus wind consists mainly of H_2 and a little He, the average molecular weight of the gas in the torus increases. If $q_m(\mathrm{He}/H_2)$ is the ratio by mass between He and H_2 we get, according to Section 5.4 (i.e., with a Maxwellian velocity distribution) for the ratio $q_d(\mathrm{He}/\mathrm{H}_2)$ of mass between He and H_2 in the torus wind

$$q_d(\mathrm{He}/\mathrm{H}_2) = c_d q_m(\mathrm{He}/\mathrm{H}_2), \tag{62}$$

where c_d has a value of about 0.06. Due to the plasma outside the gas torus, the Maxwellian velocity distribution is only a rough approximation and we estimate $c_d \approx 0.1$ for $R > 2.2$ AU. Because we expect for $R < 2.2$ AU the dissociation of H_2 in the outermost regions of the gas torus we estimate in this case $c_d \approx 0.02$. The $\bar{m}(i)$-values were computed (see Table II) with Equation (62), the mass distribution is given in Table II, and the condensation sequence given by Lewis (1972a).

The $T(i)$-values of the gas ring – at the two points with $\vartheta = 0°, 180°$ (see (50), (51)) immediately before the turn-over – are calculated according to Equations (43a) and (43b); from this and Equations (43a) and (43b) we get the $\eta_T(i)$ of Table II. But the small diameter of the gas torus is also determined – due to its own mass – by the gravitational contraction. With the $M_D(i)$-values and their centres of gravity (see Table II), one can easily calculate from (61) the mass $M_R(R_i)$ of the subsequent gas rings. The results are given in Table II.

To determine the gravitational force caused by the mass M_R of the gas ring, a three-dimensional integration is necessary. We have done this for the mass distribution given by (22b) by numerical integration with 2×10^6 points for each of 25 η-values in the range between 60 and 1000. For small (d/R)-values (see Equation (22b)) this gravitational force is nearly directionally independent (see Figure 1). For $\eta = 400$ and $M_R/M_b = 0.01$, this force is plotted as a function of d (see Figure 11). For the abscissa of the maximum of the gravitational force function it follows that $d_m/R = 1.157/\sqrt{\eta}$. With a maximal error of 3% with $\eta \in [90; 800]$ it holds for the slope $\tilde{s}$ of the straight line going through the origin of ordinates and the maximum

$$\tilde{s}(\eta) = 0.177(M_R/M_c)\eta. \tag{63}$$

We approximate the gravitational force by this straight line in the region $d \in [0; 1.4d_m]$ (see Figure 11). We denote the effective η-value inside the small circle with radius $\tilde{d} = 1.4d_m = 1.62R/\sqrt{\eta}$ with η_c. If we approximate the average η-value outside this small circle with radius $\tilde{d}$ by $\eta_T = \sqrt{\eta_r\eta_h}$ (see Equations (22a) and (22b)), the mass inside this small circle is reduced by a factor Z. As can easily be seen, Z is given by

$$Z = 1/[1 + (\eta_c/\eta_T - 1)\exp(-1.62^2)], \tag{64}$$

making it possible to substitute ZM_R for M_R.

If we add the repelling forces (cf. Equations (6), (20) and Figure 11), we get the effective η_c-value

$$\eta_c = \eta_T(1 + 0.177(Z(M_R/M_c)\eta_c). \tag{65}$$

When the inner jet stream is captured by the planet we estimate for the gas ring: $\zeta = 0.92$ and $T_a(\vartheta = 0)/T_b(\vartheta = 0) = 0.90$. For the corresponding $\tilde{\eta}_T(i)$-value it then holds that $\tilde{\eta}_T(i) = \sqrt{\eta_r\eta_h} = \sqrt{2\zeta - 1}\cdot\eta_T(i)/0.90 \approx \eta_T(i)$. This means we can take

TABLE II

Planet	i	R_i (AU)	$M_D(i)$ between R_{i-1}, R_i in % of $M_\odot$	Centre of gravity of $M_D(i)$ (AU)	$M_R(i)$–M_p in % of $M_\odot$	$T(i)$ (K)	$\bar{m}$	$\eta_T(i)$	$\eta_c(i)$	$\frac{\omega_1 - \omega_2}{\omega_1} \times 100$	$\Delta s/\Delta R$	$q_T(i)$
Neptune	1	30.06	0.4	50	0.3112	50.98	2.43	84.61	88.73	7.273	0.0918	
Uranus	2	19.18	0.45	24	0.6547	60.35	2.46	113.4	130.35	5.736	0.1512	0.400
Saturn	3	9.54	0.8	13	1.1400	101.0	2.48	137.3	188.08	4.211	2.185	0.227
Jupiter	4	5.20	1.2	6.7	1.8348	176.7	2.51	145.8	263.8	2.555	23.32	0.218
Ceres	5	2.77	0.9	3.9	2.2042	326.8	2.58	152.1	334.8	1.490	4×10^{-5}	0.148
Mars	6	1.523	0.6	2.1	2.1916	551.4	2.69	170.9	425.5	0.773	0.109	0.172
Earth	7	1.000	0.3	1.25	2.0764	772	2.82	194.9	535.1	0.2684	9.450	0.248
Venus	8	0.723	0.2	0.86	1.9788	1000.7	2.92	215.4	635.4	−0.0641	(147)	0.236
(Sun)	9	(0.00465)	0.15	0.6	(0.2089)							

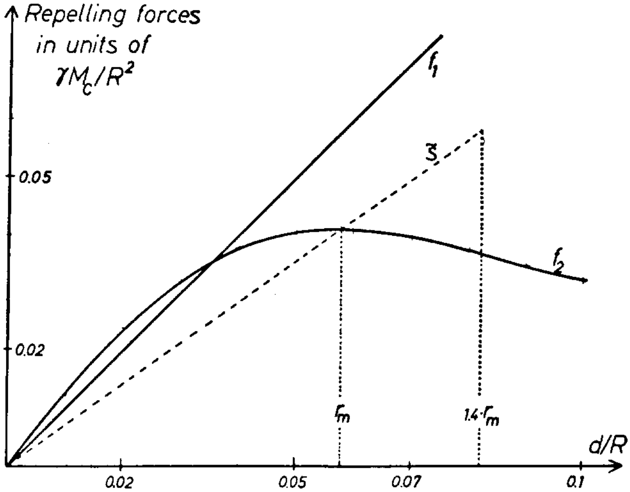

Fig. 11. Repelling forces towards the centre of the small circle of the gas torus. The force f_1 is caused by M_c and given by Equations (6), (20; $\zeta = 1$). The force f_2 originates from the gravitational attraction of the gas torus' own mass M_R. This force function f_2 is shown for $\eta = 400$, $\zeta = 1$ and $M_R = 0.01 M_c$. In the region $[0; 1.4 r_m]$ we approximate f_2 by the straight line with the slope $\tilde{s}$.

the same $\eta_T(i)$- and $\eta_c(i)$-values as if $\zeta = 1$ and $T = T(i)$, given by Equations (43a) and (43b) as

$$\eta_c(i) = \eta_T(i)/(1 - 0.177 Z \eta_T(i) M_R(i)/M_c). \tag{66}$$

These $\eta_c(i)$-values are summarized in Table II.

6.2. Capture situations for the individual planets

Now we want to determine the capture situations (see Section 5.14) of the inner rings for the individual planets relative to each other. This can only be done precisely by calculating the trajectories of the capturable gas and solid bodies within the gravitational field of the central body and the gas torus. But for our purpose the following rough analysis is sufficient (see Figure 12).

We assume that the planet with mass M_p is moving on a circle with radius $R + \Delta R$ and angular velocity ω_2. The motion of a capturable mass Δm is approximated as follows: if this mass is not in the vicinity of the planet, it is moving on a circle with radius R and angular velocity ω_1; the inclination angle α of its orbit to the planets' orbit also depends, of course, on η_c and we estimate that

$$\alpha = (50/\sqrt{\eta_c})^\circ . \tag{67}$$

The distance to the planetary orbit is given by Equation (50) ($\Delta R = r_0$). A capture can only take place if not only the planet, but also the mass Δm, are in the vicinity of the section line of both orbits (see Figure 12).

We take, as a corotating reference plane, A_c, which is perpendicular to the planetary

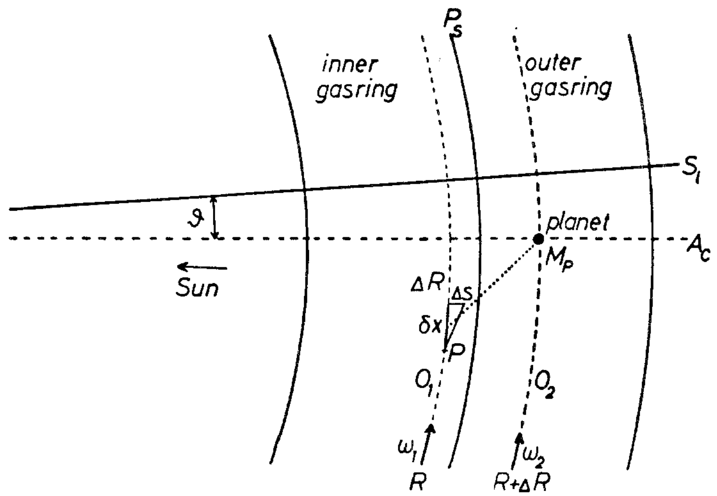

Fig. 12. Capture situations for the individual planets: O_1 is the orbit of the capturable mass Δm and O_2 is the planet's orbit. P_s is the plane of separation between the inner and outer gas ring. A_c denotes the corotating reference plane. S_l is the section line between the inner and outer gas ring as well as between the planes of O_1 and O_2. As a criterion for the capture situation we take the relative radial distance $\Delta s/\Delta R$.

orbit and includes M_c as well as the rotating planet. We now consider the following capture situation. The capturable mass Δm has moved on a circle up to the point P (see Figure 12), which is at a distance ΔR from the rotating plane A_c; furthermore, the angle ϑ between A_c and the section line of both orbits is smaller than 10°. We estimate that

$$\Delta R = 0.5R/\sqrt{\eta_c} \lessgtr D \tag{68}$$

(see Figures 8a and 8b). Then it holds that $r(\vartheta)$ can be substituted by r_0 (see Equation (50)) with an error of less than 4%. The acceleration a_p caused by the planet which acts on the mass Δm in a radial direction when it is at point P is then given by

$$a_p = (1/\sqrt{2})\gamma M_p/(2\Delta R^2). \tag{69}$$

The time t which the mass Δm needs to cover the distance δx (see Figure 12) in our corotating system is then given by

$$t = (\delta x/R)/(\omega_1 - \omega_2). \tag{70}$$

As a criterion for the capture situation we take the relative distance $(\Delta s/\Delta R) = 0.5a_p t^2/\Delta R$ which the mass Δm has covered in the time t in a radial direction. With $\delta x/\Delta R = \text{const.} \ll 1$, and with $\omega = (\gamma M_{\text{eff}}(R)/R^3)^{0.5}$, we get (cf. Equation (68))

$$\Delta s/\Delta R \sim M_p\sqrt{\eta_c}/[\sqrt{M_{\text{eff}}(R)} - \sqrt{M_{\text{eff}}(R + \Delta R)}/(1 + \Delta R/R)^{1.5}]^2, \tag{71}$$

where the proportional factor is $(\delta x/\Delta R)^2/\sqrt{32}$. Because it is simpler and also plausible, we assume that during the capture process the inner matter band is within the centre of the whole librating gas torus. To a good approximation we can, for $|\vartheta| < 10°$, ignore the swinging of the gas torus for the determination of the effective mass. Our computer calculation leads to

$$M_{\text{eff}}(R + 0.5R/\sqrt{\eta_c}) = M_{\text{eff}}(R) + 0.142Z(M_R/M_c)\sqrt{\eta_c}, \tag{72}$$

with Z from Equation (64) and $M_{\text{eff}}(R) \approx M_c + M_R$. The results of $\Delta s/\Delta R$ without the proportional factor are listed in Table II.

For the inner planets the capture situation for $\vartheta > 10°$ is more adverse than for the outer planets. The reason for this is that Equation (72) holds only for small values of $|\vartheta|$ or $|\vartheta - 180°|$. Outside these regions $(\omega_1 - \omega_2)/\omega_1$ does not change very much for the outer planets, but it enlarges considerably for the inner planets. If we take this into account we can interpret our calculated $(\Delta s/\Delta R)$-values in the following way:

(1) Neptune and Mars captured only a small amount of matter in a retrograde direction.
(2) Uranus captured a greater amount of matter in a retrograde direction.
(3) Earth and Saturn have captured the matter of the inner gas ring in a prograde direction; because their capture situations are equivalent we expect that the primordial Earth system was similar to the Saturnian satellite system.
(4) Jupiter has collected the matter of the inner gas ring in a prograde direction, but also Jupiter is that planet which has collected by far most of the solid matter from the gas disk. We suggest that the perturbed planetesimals have swept up solid matter from the cool gas disk excluding a disk region with a radius of about 1.4 AU, so we expect that it has the smallest inclination of equator to orbit of all planets.
(5) We get quite a different capture situation for Venus, because of $\omega_1 - \omega_2 < 0$. A capture does not seem to be possible; thus we expect the formation of an 'accompanying' planet (Mercury) in the inner gas ring. Due to the strong gravitational interaction with Venus (note the high $\Delta s/\Delta R$-value in Table II), Mercury has lost a portion of its angular momentum. This brings about its elliptical orbit. It is conjectured that Mercury has lost a further part of its angular momentum due to friction with the contracting gas torus.

This result for the capture situations of the planets is relatively independent of the parameters we have chosen: e.g. we can reduce the masses $M_D(i)$ and the temperatures $T(i)$ in Table II by 20% and enlarge ΔR (cf. Equation (68)) by 50% to get the same results.

6.3. Spin and Spin Axis of the Planets

According to Section 5.15 one gets the spin axes of the planets by adding the vectors $\vec{S}_0$ and $\vec{S}_i$. If, according to Section 5.15, all three successive phases have occurred, one has of course two vectors $\vec{S}_i$: a small one S_i(II) of phase II, where the growing planet has captured the matter in the retrograde direction, and a great one S_i(III) belonging to phase III.

The vector model we use here according to Section 5.15 is defined by: The angles between equator to orbit are, for $\vec{S}_o$, 0° and for S_i in the case of a retrograde capture 145° and a prograde capture −35°. The spin S_o is smaller the more gas a planet has captured in relation to solid matter. Further, it depends on the ε-values of the orbits of the captured planetesimals. For the inner planets the ε-values are relatively small because here the friction with dense gas in the gas rings is high – especially for Venus, which is probably the reason for its retrograde spin (cf. A. and A, 1970b), but this may also be caused by $\omega_1 < \omega_2$ (see Figure 12 and Table II). Further, the relation between the escape velocity from the planets and their orbital velocities is small compared to the outer planets. Yet to get a simple qualitative vector model we put the relative spins $\hat{S}_o = S_o/\theta_p$, where θ_p is the present moment of inertia of the planets, constant except for Earth and Saturn, where we reduce the constant by a factor of $\frac{2}{3}$. Together with the relative spins $\hat{S}_i = S_i/\theta_p$ we get the vector model of Figure 13 for the capture situations of Mars, Neptune; Uranus; Earth, Saturn.

The final relative spin $\hat{S}_p = S_p/\theta_p = \omega_p$ of each planet is not (cf. Section 5.15) $|\vec{S}_o + \vec{S}_i|$ but the sum of the small primordial spin $\hat{S}_{pa}$ of the planet with its atmosphere and of the angular momentum of $\hat{S}_r$, which the gas ring has when it is absorbed (see Figure 13). That means the spin $S_p < |\vec{S}_o + \vec{S}_i|$; this reduction is not great for these planets with a relatively small gas disk (Mars, Neptune), but for those planets

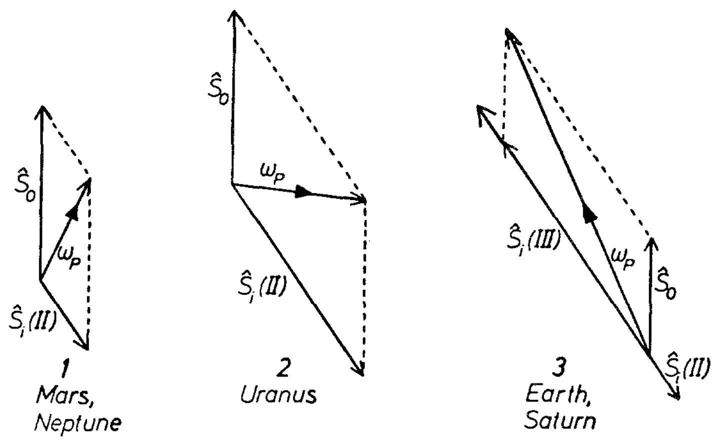

Fig. 13. Vector model for the capture situations (1), (2), (3) of Section 6.2. $\vec{S}_o$ is parallel to the orbital angular momentum $\vec{A}_o$. The angle between $\vec{A}_o$ and $\vec{S}_i$(II) (= retrograde capture) is 135° and with S_i(III) (= prograde capture) is −35°. The total spin $\vec{S}_i + \vec{S}_o$ is reduced by the main process to the planetary spin S_p. To get the angular velocity $\omega_p = S_p/\theta_p$ of the planets, all spins S_p, S_i, S_o are divided by θ_p so we get $\hat{S}_p$, $\hat{S}_i$, $\hat{S}_o$.

A better and more correct vector model we get by the following: The angles with $\vec{A}_o$ are for $\vec{S}_o$ 10°, $\vec{S}_i$(II) 150° and S_i(III) 30°; $\vec{A}_o$, $\vec{S}_o$ and $\vec{S}_i$(III) are within the same plane, but the angle between this plane and the plane subtended by $\vec{A}_o$ and $\vec{S}_i$(II) is about 90°.

with a relatively great original gas disk such as Jupiter, Saturn, and Earth. Also, if one takes this into account, then, for the spin periods $\sim 1/\omega_p$ of Jupiter (9.8^h), Saturn (10.2^h) and the original angular velocity of the Earth, one expects values smaller than for Mars (24.6^h), Uranus, Neptune (here recent measurements from the Kitt-Peak Observatory yielded Uranus 23^h and Neptune 22^h).

The results of Sections 6.2 and 6.3 are summarized in Table I.

6.4. The semi-major axes of the planets

Because the turn-over process depends on the building up of a libration, we expect exactly a geometric series for the R_i-values, if $(r_T/R) \sim 1/\sqrt{\eta}$ is constant. The $\eta(i)$-values with regard to the turn-over process depend not only on $\eta_c(i)$ but also somewhat on $\eta_T(i)$; so we take

$$\eta(i) = \eta_T(i)^{0.25}\eta_c(i)^{0.75}. \tag{73}$$

According to Table II, these $\eta(i)$-values get smaller with decreasing R-values; this means the turn-over ensues faster, i.e. the R_{i-1}/R_i-values get smaller.

But there are three exceptions: for $i = 2$ (Uranus) the R_1/R_2-value $(=1.57)$ is relatively small (incompatible with Titius–Bode's 'law') and for $i = 5.6$ (Asteroides, Mars) these values are relatively large (1.88, 1.82). Yet the speed at which the turn-over process occurs also depends on the relation between the libration amplitude of the $(i-1)$th turn-over to the ith turn-over. The reason for this is that a fixed portion of the vertical libration always remains (see Figure 7); the greater this libration amplitude in relation to the critical amplitude for the next turn-over, the faster of course does the turn-over occur. The relative change q_T of the libration amplitude $l_a \sim 1/\sqrt{\eta}$ is given by $l_a^{-1}R \operatorname{grad} l_a = \sqrt{\eta}\, R \operatorname{grad}(1/\sqrt{\eta})$. So, for the relative change from the $(i-1)$th to the ith turn-over, with Equation (73), we obtain

$$q_T(i) = (\eta(i-1)\eta(i))^{0.25} \times$$
$$\times\ (R(i-1)R(i))^{0.5}\,\frac{1/\sqrt{\eta(i-1)} - 1/\sqrt{\eta(i)}}{R(i-1) - R(i)}. \tag{74}$$

The $q_T(i)$-values are listed in Table II. With these $q_T(i)$-values we can understand immediately the three 'exceptions'. For $i = 2$, q_T has the greatest value, which means the turn-over occurs relatively fast; and for $i = 5.6$ we have the smallest q_T-values, which means the R_{i-1}/R_i-values are relatively large. Thus, we get the correct quantitative result for all semi-major axes of the regular planets.

As A and A (1970a) and Birn (1973) have pointed out, it is very improbable that the R_i-values have changed very much after the formation of the planetary system.

6.5. Mass ratios

Here we give only simple applications for our four systems (planetary, Jovian, Saturnian and Uranian system). Because the greatest secondary bodies have collected solid matter from the inside gas disk, we expect that the next – but *not* the previous –

secondary bodies to be formed are unexpectedly small or they have not been formed at all. This is true for all four systems.

Further, we expect that the outermost regular secondary bodies (Neptune, Callisto, Titan, Oberon) have a surprisingly great mass. This is also true. There are two reasons for this: the first is that only here does the building up of the libration begin 'at zero' which means that the contraction of the gas torus was greater here than it was for all other secondary bodies; and the second is that only here was there no mass loss caused by the collection of solid matter by the next outer secondary body.

Further, this theory can explain the mass ratios between satellite systems and the planets. The first principle is, therefore, that the better the capture situation, the greater the mass ratio between the regular satellites and the planets. This is true for the capture situations (1), (2) and (3) in Section 6.2. Further, we have to take into account that the decrease in temperature due to turn-over is greatest for small R-values. Therefore, the mass of the condensed matter of the inner gas ring is high here in relation to the allied planet's mass (Mercury/Venus = 0.068; Moon/Earth = 0.012; sum of the Saturnian satellites/Saturn = 0.0031).

The reason the mass ratio Triton/Neptune = 0.0033 is relatively great is that Neptune has collected only a small quantity of gas due to the small $M_R(1)$-value (see Table II); we suggest that this is also the reason for its relatively high density.

6.6. The formation of the Saturnian rings

When the gas ring comes into the outer region of Saturn's atmosphere, the inner part of the gas ring is braked. We expect a short intensive heating of the gas and a short period of intensive shock waves. By this a great quantity of plasma outside the gas ring is formed which is, by Equation (48), shifted outwards because it enters a state of partial corotation. Within a short period the gas ring is absorbed by the atmosphere and this enlarges the rotational velocity of Saturn.

We agree with the formation process of the Saturnian rings proposed by A and A (1973) and Alfvén (1976). This means that the plasma condensed and, according to the two-thirds law, the grains produced by the condensation fell down to two-thirds of their original central distances. We believe that A and A's formation process of the Saturnian rings can be understood very well in the framework of this theory because (1) it is clear that there is no neutral gas in the central plane, which would thoroughly disturb the two-thirds law because of friction with the small condensed infalling grains (see Equation (57)) and (2) it is necessary that Janus and Mimas were already in existence.

Acknowledgements

I wish to thank Prof. W. Deinzer, Dr J. Hardorp, Prof. H.-H. Voigt and Dr A. Wittmann for their interest and encouragement; furthermore, I am obliged to Dr A. Wittmann for reviewing the manuscript. The support of this work by Prof. W. A. Bingel is gratefully acknowledged.

References

Alfvén, H. and Arrhenius, G.: 1970a, *Astrophys. Space Sci.* **8**, 338.
Alfvén, H. and Arrhenius, G.: 1970b, *Astrophys. Space Sci.* **9**, 3.
Alfvén, H. and Arrhenius, G.: 1973, *Astrophys. Space Sci.* **21**, 117.
Alfvén, H. and Arrhenius, G.: 1974, *Astrophys. Space Sci.* **29**, 63.
Alfvén, H.: 1976, *Astrophys. Space Sci.* **43**, 97.
Allen, C. W.: 1973, *Astrophysical Quantities* (3rd edn.), The Athlone Press.
Anders, E.: 1971, *Ann. Rev. Astron. Astrophys.* **9**, 1.
Brecher, A.: 1972, *Nice Conference, Symp. Origin of the Solar System*, Edition du Centre Nationale de la Recherche Scientifique, Paris, p. 260.
Birn, J.: 1973, *Astron. Astrophys.* **24**, 283.
Cameron, A. G. W.: 1972, *Nice Conference, Symp. Origin of the Solar System*, Edition du Centre Nationale de la Recherche Scientifique, Paris, p. 56.
Cameron, A. G. W.: 1973, *Icarus* **18**, 407.
Cameron, A. G. W.: 1975, *Icarus* **25**, 588.
Danielsson, L.: 1973, *Astrophys. Space Sci.* **24**, 459.
Dole, S. H.: 1962, *Planetary Space Sci.* **9**, 541.
Glasstone, S.: 1965, *Sourcebook on the Space Sciences*, Van Nostrand Company, p. 341.
Handbury, M. J. and Williams, J. P.: 1976, *The Observatory* **96**, 140.
Giuli, R. T.: 1968a, *Icarus* **8**, 301.
Giuli, R. T.: 1968b, *Icarus* **9**, 186.
Larson, R. B.: 1972, *Nice Conference, Symp. Origin of the Solar System*, Edition du Centre Nationale de la Recherche Scientifique, Paris, p. 142.
Lewis, J. S.: 1972a, *Icarus* **16**, 241.
Lewis, J. S.: 1972b, *Nice Conference, Symp. Origin of the Solar System*, Edition du Centre Nationale de la Recherche Scientifique, Paris, p. 202.
Lewis, J. S.: 1973, *Technology Review*, Massachusetts Institute of Technology, **76**, 20.
Marcus, A. H.: 1967, *Icarus* **7**, 283.
Mestel, L.: 1972, *Nice Conference, Symp. Origin of the Solar System*, Edition du Centre Nationale de la Recherche Scientifique, Paris, p. 21.
Newburn, R. L., Jr. and Gulkis, S.: 1973, *Space Sci. Rev.* **14**, 179.
Safronov, V. S.: 1972, *Nice Conference, Symp. Origin of the Solar System*, Edition du Centre Nationale de la Recherche Scientifique, Paris, p. 89.
Safronov, V. S. and Zvjagina, E. V.: 1969, *Icarus* **10**, 109.
Schmitt, Harrison H.: 1975, *Space Sci. Rev.* **3**, 259.
ter Haar, D.: 1972, *Nice Conference, Symp. Origin of the Solar System*, Edition du Centre Nationale de la Recherche Scientifique, Paris, p. 71.
Urey, H. C.: 1972, *Ann. New York Acad. Sci.* **194**, 35.
Whipple, F. L., Lecar, M. and Franklin, F. A.: 1972 *Nice Conference, Symp. Origin of the Solar System*, Edition du Centre Nationale de la Recherche Scientifique, Paris, p. 312.